

Ballistocardiography and Seismocardiography: A Review of Recent Advances

Omer T. Inan, *Member, IEEE*, Pierre-Francois Migeotte, *Member, IEEE*, Kwang-Suk Park, *Senior Member, IEEE*,
Mozziyar Etemadi, *Student Member, IEEE*, Kouhyar Tavakolian, *Member, IEEE*, Ramon Casanella, *Member, IEEE*,
John Zanetti, Jens Tank, Irina Funtova, G. Kim Prisk, *Senior Member, IEEE*, and Marco Di Rienzo, *Member, IEEE*

Abstract—In the past decade, there has been a resurgence in the field of unobtrusive cardiomechanical assessment, through advancing methods for measuring and interpreting ballistocardiogram (BCG) and seismocardiogram (SCG) signals. Novel instrumentation solutions have enabled BCG and SCG measurement outside of clinical settings, in the home, in the field, and even in microgravity. Customized signal processing algorithms have led to reduced measurement noise, clinically relevant feature extraction, and signal modeling. Finally, human subjects physiology studies have been conducted using these novel instruments and signal processing tools with promising clinically relevant results. This paper reviews the recent advances in these areas of modern BCG and SCG research.

Index Terms—Ballistocardiogram (BCG), cardiomechanical signals, noninvasive physiologic monitoring, seismocardiogram (SCG), ubiquitous health.

Manuscript received May 14, 2014; revised August 20, 2014; accepted September 29, 2014. Date of publication; date of current version. The work of P. F. Migeotte was supported by the Belgian Federal Science Policy Office via the European Space Agency PRODEX program (ILSRA-2009-0729). The work of G. K. Prisk was supported by the National Space Biomedical Research Institute through NASA NCC9-58. The work of J. Tank and I. I. Funtova were supported by the German Space Agency (DLR) under Grant 50WB1117. The work of M. Di Rienzo was supported in part by the Italian Space Agency through ASI 2013-061-I.0 and ASI 2013-079-R.0.

O. T. Inan is with the School of Electrical and Computer Engineering, Georgia Institute of Technology, Atlanta, GA 30308 USA (e-mail: oeinan@gmail.com).

P.-F. Migeotte is with the Department of Cardiology, Universite Libre de Bruxelles 1050, Brussels, Belgium (e-mail: Pierre-Francois.Migeotte@ulb.ac.be).

K.-S. Park is with the Department of Biomedical Engineering, Seoul National University, Seoul 110-799, Korea (e-mail: kspark@bmsil.snu.ac.kr).

M. Etemadi is with the Department of Bioengineering and Therapeutic Sciences, University of California at San Francisco, San Francisco, CA 94143 USA (e-mail: mozziyar.emetadi@ucsf.edu).

K. Tavakolian is with the Department of Electrical Engineering, University of North Dakota, Grand Forks, ND 58202 USA (e-mail: kouhyart@gmail.com).

R. Casanella is with the Instrumentation, Sensors, and Interfaces Group, Universitat Politècnica de Catalunya, 08034 Barcelona, Spain (e-mail: ramon.casanella@upc.edu).

J. Zanetti is with Acceleron Medical Systems, Arkansaw, WI 54721 USA (e-mail: jmzsenior@gmail.com).

J. Tank is with the Klinische Pharmakologie, Medizinische Hochschule Hannover, 30625 Hannover, Germany (e-mail: Tank.Jens@mh-hannover.de).

I. Funtova is with the Laboratory for Autonomic Regulation of Cardiorespiratory System, Institute of Biomedical Problems, Russian Academy of Sciences, 123007 Moscow, Russian (e-mail: funtova.imbp@mail.ru).

G. K. Prisk is with the Department of Medicine and Radiology, University of California at San Diego, La Jolla, CA, 92093 USA (e-mail: kprisk@ucsd.edu).

M. Di Rienzo is with the Department of Biomedical Technology, Fondazione Don Carlo Gnocchi, ONLUS, 20133 Milano, Italy (e-mail: mdrienzio@dongnocchi.it).

Color versions of one or more of the figures in this paper are available online at <http://ieeexplore.ieee.org>.

Digital Object Identifier 10.1109/JBHI.2014.2361732

I. INTRODUCTION

As detailed in the following sections, the ballistocardiogram (BCG) is a measurement of the recoil forces of the body in reaction to cardiac ejection of blood into the vasculature [1], while the seismocardiogram (SCG) represents the local vibrations of the chest wall in response to the heartbeat [2]. The BCG phenomenon was first observed in 1877 by Gordon, with the finding that, as a subject would stand on a weighing scale, the needle would vibrate synchronously to the subject's heartbeat [3]. Nearly 60 years later, Starr and colleagues created an instrument in the form of a table with a mobile top surface to measure the BCG in a repeatable scientific manner [1]. The SCG was first observed by Bozhenko in 1961, and was first applied in clinical studies 30 years later in 1991 by Salerno and Zanetti [4]. Throughout the 1900s, both BCG and SCG signals were heavily investigated and several publications appeared in major scientific and clinical journals (e.g., [4]–[7]). However, because of the advent of echocardiography and magnetic resonance imaging, and overly-cumbersome hardware, BCG and SCG were largely abandoned by the medical community [8].

Today, technological advancements largely simplify the measurement and assessment of these signals and open new perspectives in their clinical use. This paper reviews the instrumentation and signal processing advances which have helped to propel BCG and SCG into this revival. It also summarizes some of the key human subjects studies performed recently that support the use of BCG and SCG in extra-clinical applications.

II. DESCRIPTION OF BCG AND SCG SIGNALS

A. BCG Signal Description

At every heartbeat, the blood travelling along the vascular tree produces changes in the body center of mass. Body micromovements are then produced by the recoil forces to maintain the overall momentum. The BCG is the recording of these movements, can be measured as a displacement, velocity, or acceleration signal, and is known to include movements in all three axes. The longitudinal BCG is a measure of the head-to-foot deflections of the body, while the transverse BCG represents antero-posterior (or dorso-ventral) vibrations. The original bed- and table-based BCG systems focused on longitudinal BCG measurements, representing what was supposed to be the largest projection of the 3-D forces resulting from cardiac ejection [1]. Table I summarizes modern BCG measurement systems and their axes of measurement. Note that for some systems, head-to-foot and dorso-ventral forces are unavoidably, mixed

TABLE I
MODERN BCG SYSTEMS AND THEIR CORRESPONDING MEASUREMENT AXES

Modern BCG System	Axis	Comments / Challenges
Accel. (0g)	All (3-D)	- Needs reduced gravity
Accel. (1g)	Head-to-foot	- Placement affects signal shape and amplitude - Motion artifacts must be detected and mitigated
Bed	Head-to-foot or Dorsio-ventral	- Cross-axis coupling - Changes in sleep position affect signal quality / shape
Chair	Head-to-foot or Dorsio-ventral	- Posture affects signal quality and repeatability
Weighing Scale	Head-to-foot	- Posture affects signal quality and repeatability - Motion artifacts must be detected and mitigated

66 together in the measurement, and this should be accounted for
67 when interpreting results. However, in spite of the 3-D nature of
68 the BCG, for a long period of time only the microdisplacements
69 of the body along the longitudinal axis (head-to-foot) were con-
70 sidered. Currently, BCG is mainly measured using a force plate
71 or force sensor placed on a weighing scale or under the seat of a
72 chair, with the subject in a vertical position. Modern approaches
73 to BCG measurement are discussed below in Section III.

74 It should be considered, however, that the gravity force and
75 any contact of the body with external objects, including the
76 floor and measuring devices, somewhat interferes with, or even
77 impedes, the body displacement induced by the recoil forces.
78 As a result, the BCG measurement on earth is always affected
79 by some distortion. The ideal environment for assessing the
80 BCG would be in microgravity settings, such as during space
81 missions. Such experiments have been performed, and the re-
82 sults described below confirm that in microgravity the whole
83 body recoil forces (BCG) are significant in all three dimensions
84 [9]–[12]. Modeling studies examining the cardiogenic traction
85 forces of the aorta have confirmed this finding as well [13].

86 B. SCG Signal Description

87 SCG is the measure of the thoracic vibrations produced by the
88 heart's contraction and the ejection of blood from the ventricles
89 into the vascular tree. Today, the SCG can readily be detected
90 by placing a low-noise accelerometer on the chest. If a tri-axial
91 accelerometer is used, SCG components are present in all three
92 axes, each displaying a specific pattern [12], [14]. However, in
93 the literature, the majority of studies on SCG only focus on the
94 amplitude of the dorso-ventral component, although it is likely
95 that additional biological information could be derived also from
96 the analysis of the longitudinal and lateral SCG components, and
97 from the analysis of the acceleration vector trajectory during
98 the heart cycle. Unless the contrary is stated to be consistent
99 with the prevalent literature only the dorso-ventral acceleration
100 component of SCG will be considered in the remainder of this
101 paper.

102 C. BCG and SCG Waveforms

103 For each heart contraction, a BCG and SCG waveform is gen-
104 erated. Each waveform is characterized by several peaks and val-

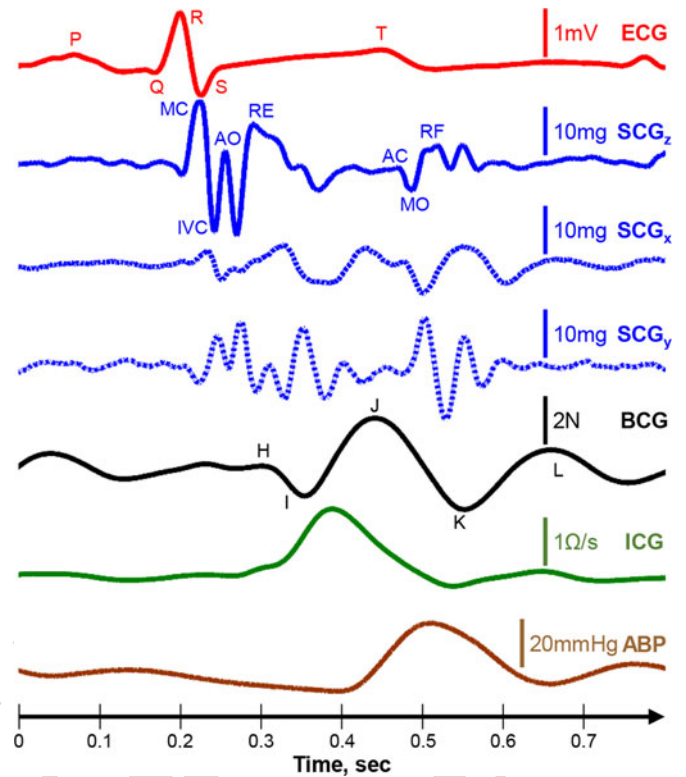


Fig. 1. Simultaneously acquired Lead II electrocardiogram (ECG); three-axis seismocardiogram (SCG) with z indicating the dorso-ventral axis, x indicating the right-to-left lateral axis, and y indicating the head-to-foot axis; ballistocardiogram (BCG); impedance cardiogram (ICG); and arterial blood pressure (ABP) measured at the finger, signals from one subject, illustrating the relative timing and amplitude features of the signals.

105 leys reflecting specific events of the beating heart. Fig. 1 shows a
106 typical ECG, head-to-foot BCG, tri-axial SCG, impedance car-
107 diogram (ICG), and arterial blood pressure (ABP) measurement
108 from a healthy subject (data were collected with approval from
109 the Institutional Review Board, IRB, at the Georgia Institute of
110 Technology, and with written informed consent obtained). A
111 high-resolution, miniature accelerometer was used for the SCG
112 data collection (356A32, PCB Piezotronics, Depew, NY, USA),
113 and a modified weighing scale was used for the BCG recording
114 as described previously in [15]. The ECG and ICG waveforms
115 were measured using the BN-RSPEC and BN-NICO wireless
116 units (BIOPAC Systems, Inc., Goleta, CA, USA) interfaced to
117 the MP150WSW data acquisition hardware (BIOPAC Systems,
118 Inc., Goleta, CA, USA). The ABP was measured from the fin-
119 ger using the A2SYS Nexfin Monitor (Edwards Lifesciences,
120 Irvine, CA, USA). For this measurement, z corresponded to the
121 dorso-ventral, y to the head-to-foot, and x to the right-to-left
122 lateral components of the SCG. The labels of the peaks and val-
123 leys of the dorso-ventral components shown in this figure are
124 according to [16], [17]; for the BCG, the labels are according
125 to [1]. For the SCG, the labels correspond to the physiological
126 event they are believed to represent: MC, mitral valve closure;
127 IVC, isovolumetric contraction; AO, aortic valve opening; RE,
128 rapid ejection; AC, aortic valve closure; MO, mitral valve open-
129 ing; and RF, rapid filling. For the BCG, the labels of the waves
130 are not associated directly with underlying events, but rather
131 the current understanding is that the waveform represents the

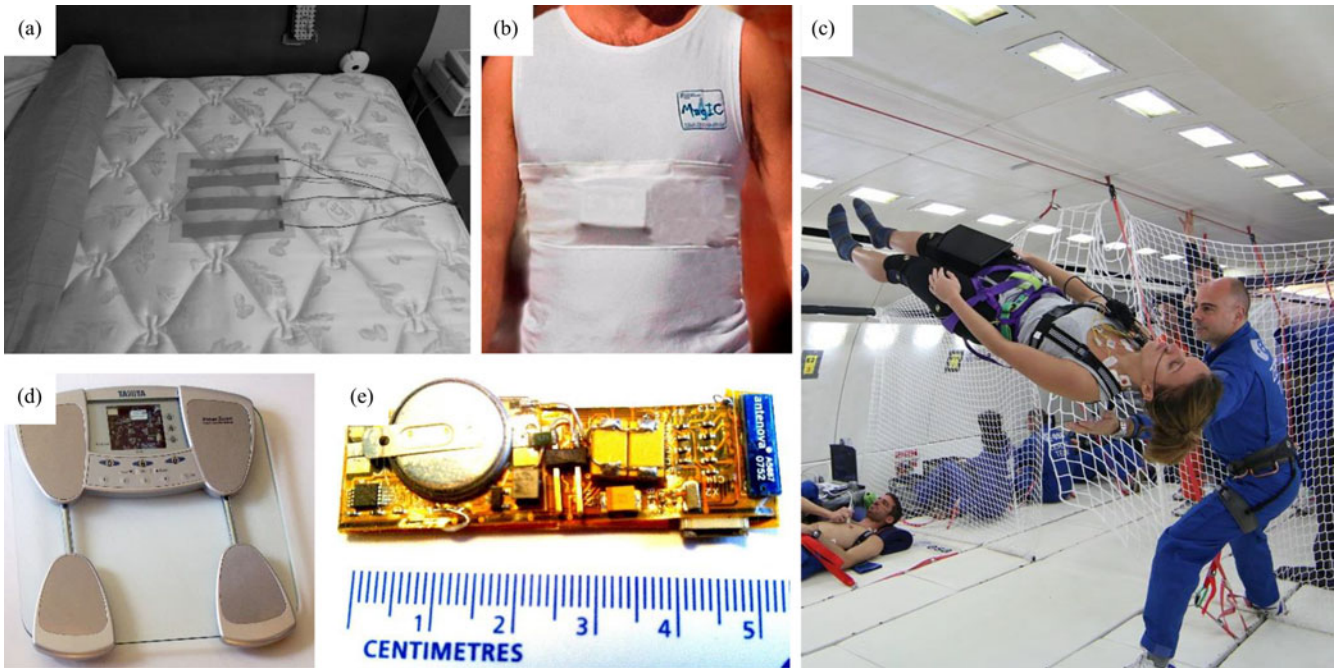


Fig. 2. Compilation of modern BCG and SCG acquisition hardware. (a) PVDF sensor installed into the bed for BCG measurements during sleep. (b) Tri-axial SCG measurement system built into the MagIC-SCG vest for continuous recordings during normal activities of daily living. Modified from [14] with permission. (c) Wearable 3-D BCG measurement hardware (Pneumocard) being used on board a parabolic flight for microgravity BCG measurements; Photo Credit: ESA. (d) Weighing scale with built in circuitry for BCG measurement from a standing subject. (e) Flexible hardware for chest-mounted tri-axial SCG measurements.

132 combined mechanical pulse response of the vasculature and
 133 body to cardiac ejection of blood [18]. Note that, when the
 134 BCG is measured by a scale or force plate, the SCG and BCG
 135 units are not the same; the SCG records the accelerations of
 136 the chest wall, and is thus presented in units of milligram; the
 137 BCG represents the displacements of the center of mass of
 138 the subject on the weighing scale, which are then converted
 139 to units of force by the spring constant for the scale platform,
 140 and thus it is presented in units of Newtons. The mass that is
 141 accelerated for the SCG is not the same as the mass acceler-
 142 ated for the BCG; as such, the direct conversion of the BCG to
 143 acceleration units or the SCG to force units has not yet been
 144 elucidated.

145 D. Importance of Sensor Location, Axis Selection 146 and Orientation

147 For both BCG and SCG, the measurement location has a sig-
 148 nificant bearing on the morphology, amplitude, and clinically
 149 relevant features of the signal. For the SCG, since it is a mea-
 150 sure of local vibrations, the precise location of the sensor on
 151 the chest impacts the measured signal [19]–[21]. A widely used
 152 placement has been on the sternum [14], [22], [23]. Pandia *et al.*
 153 found that the second heart sound was more pronounced when
 154 the SCG was measured on the left side of the chest compared
 155 to the sternum [19]. For BCG signals measured using an ac-
 156 celerometer, the same is true; an accelerometer placed on the
 157 foot will not measure the same BCG signal as one placed on
 158 the head, thus stressing the importance of a clear description of,
 159 and thoughtfulness regarding, the sensor location on the body.

An additional crucial issue is the orientation of the acceleration
 axis. BCG or SCG accelerations in the dorso–ventral direction
 will not be identical to those in the lateral (right-to-left) or head-
 to-foot direction; consequently, depending on the purpose of
 the measurement the axis should be chosen accordingly or a
 three-axis accelerometer should be used.

In spite of the major role played by the selection of the mea-
 surement axes, the axes orientation, and the sensor location,
 from the review of the existing literature it appears that infor-
 mation on these aspects is often missing, making difficult the
 understanding of the experimental setup and the interpretation
 of results. Thus, as detailed in Section VI, a standardization
 on these issues is deemed necessary, and in the meantime, it
 is advisable that the above pieces of information are clearly
 stated in any scientific communication dealing with BCG and
 SCG.

III. INSTRUMENTATION: ENABLING UBIQUITOUS MONITORING

Fig. 2 shows a compilation of photos depicting several exam-
 ples of modern BCG and SCG acquisition hardware, enabling
 data acquisition in a variety of settings, including in bed, in
 the home, outdoors, and in microgravity. These systems are
 discussed below in detail.

A. Wearable BCG or SCG Systems

The primary advantage of wearable BCG or SCG mea-
 surement systems is the possibility of obtaining data contin-
 uously throughout normal daily living. Additionally, record-
 ings with wearable systems can potentially be acquired in any

187 environment; thus, providing an opportunity to assess a per-
 188 son's cardiovascular performance under various environmental
 189 settings or stressors.

190 The sensor type used most often for wearable BCG or SCG
 191 measurements is an accelerometer, typically with three-axis
 192 measurement capability, that is mechanically coupled to the
 193 body with either adhesives, plastic mounting, or textiles. In
 194 2007, Castiglioni *et al.* tested the SCG assessment by an ex-
 195 ternal three-axis MEMS accelerometer placed on the left clavi-
 196 cle, connected to a smart garment with textile ECG electrodes,
 197 thus obtaining simultaneous tri-axial SCG and single-lead ECG
 198 recordings [24]. The concept was subsequently refined, and in
 199 2010, Di Rienzo *et al.* proposed an integrated vest equipped with
 200 sensors, the MagIC-SCG device, in which the accelerometer
 201 was inside the system electronics and placed in contact with the
 202 subject's sternum [14]. Through this system, SCG was recorded
 203 over 24 h in ambulant subjects, while performing a variety of
 204 activities of normal daily living and beat-to-beat estimates of
 205 cardiac time intervals (CTIs) could be estimated [21]. Chuo
 206 *et al.* developed miniaturized hardware ($55 \times 15 \times 3$ mm) on
 207 a flexible substrate with adhesive backing for wireless tri-axial
 208 SCG recording from the sternum (also with a MEMS accelerom-
 209 eter) together with single-lead ECG and coarse single-point skin
 210 temperature via a thermistor [25]. Baevsky *et al.* developed a
 211 portable system, "Pneumocard," for the assessment of the car-
 212 diac function of cosmonauts on board the International Space
 213 Station [26]. The system comprised a single-axis MEMS ac-
 214 celerometer placed at the apex of the heart for the recording of
 215 the SCG signal. Later, a three-axis MEMS accelerometer was
 216 added to the system for the recording of the BCG signal. The
 217 accelerometer was placed on the back of the subject, either at
 218 the center of mass or between the scapulae and its performance
 219 during the microgravity phases of parabolic flights was tested
 220 by Migeotte *et al.* [27]–[29].

221 He *et al.* placed a tri-axial MEMS accelerometer for BCG
 222 measurement in a plastic mount over the ear, with auxiliary
 223 sensors include for ECG and / or photoplethysmogram (PPG)
 224 measurement, respectively, [30], [31]. Hyun *et al.* used an
 225 electromagnetic film (EMFi) patch to measure the vibrations
 226 of the chest wall in the dorso-ventral direction (transverse);
 227 however, it should be noted that the exact position on the
 228 chest for the measurement was not provided, and on the ba-
 229 sis of morphology, while the signal was called the BCG, it
 230 was likely rather an SCG [32]. Another notable approach—
 231 that is not exactly a wearable device, but provides some similar
 232 advantages—was demonstrated by Balakrishnan *et al.* with the
 233 head-to-foot (longitudinal) direction ballistocardiographic dis-
 234 placements of the head being captured and processed from video
 235 recordings [33].

236 B. Weighing Scale BCG

237 The first measurement of BCG on an electronic scale was
 238 demonstrated in 1990 by Jim Williams of Linear Technology, as
 239 described in his application note AN-43 [34]. Williams built an
 240 elegant circuit capable of measuring bodyweight with tremen-
 241 dous accuracy—4.5 g resolution up to 136 kg—and found mo-

tion artifacts, and the BCG as the largest sources of noise for
 his measurements.

242 The main advantage with weighing-scale-based BCG mea-
 243 surement is that the subject is standing up for the measurement—
 244 ironically, this is also the main disadvantage. While the standing
 245 posture of the subject is ideal for ensuring that the measurement
 246 is purely longitudinal, it also means the measurements are sus-
 247 ceptible to motion artifacts and floor vibrations. This also places
 248 a practical limit on the duration of the measurements, as the pa-
 249 tient will likely only stand still on the scale for 30–60 s at a time at
 250 most. Another key advantage of these systems is that they lever-
 251 age the tremendous popularity of weighing scales, with more
 252 than 80% of American households owning a scale, and multiple
 253 companies developing new and improved "smart" scales with
 254 enhanced capabilities. The scale is also used by heart failure pa-
 255 tients at home to monitor increasing trends in their bodyweight,
 256 which may be related to increased fluid retention [35], [36].

257 With these potential advantages in mind, researchers have
 258 rigorously investigated this mode of BCG measurement. Inan
 259 *et al.* measured the mechanical frequency response of several
 260 commercially available scales at various loads to determine if
 261 the bandwidth was sufficient for BCG recording over a wide
 262 range of bodyweight. For bodyweights up to 160 kg, they found
 263 that the mechanical systems of most commercial scales have
 264 a bandwidth exceeding 15 Hz, which is sufficient for BCG
 265 measurement [15]. Note that for preserving the accuracy of
 266 time interval detection from the BCG, such as the R–J interval
 267 between the ECG and BCG, analog and digital low-pass filtering
 268 operations should not use a cutoff frequency lower than 25 Hz
 269 [37]. BCG measurement on a scale has also been successfully
 270 demonstrated by Gonzalez-Landaeta *et al.* [38] and Shin *et al.*
 271 [39], and in all studies the shape and amplitude of the signal is
 272 very similar to the traditional BCG recordings taken by Starr
 273 *et al.* nearly a century earlier [1].

276 C. Bed-Based BCG Systems

277 BCG can be applied in evaluating the sleep stages and sleep
 278 related disorders in more comfortable environment replacing
 279 some functions done by polysomnography (PSG). Since BCG-
 280 based technology does not require attaching electrodes on pa-
 281 tient body surface, it has advantage over ECG of not disturb-
 282 ing subject's ordinary sleep behaviors in collecting data. BCG
 283 measurement can be integrated with the subject's sleeping en-
 284 vironment using several types of sensors, the first of which was
 285 a static charge sensitive bed by Alihanka *et al.* [40], and more
 286 recently the following implementations: Pressure sensor in the
 287 air mattress [41] or in pad [42], film-type force sensors [43] or
 288 load cells in the legs of bed [44], microbend fiber optic BCG
 289 sensor [45]–[47], EMFi sensors [48], piezoelectric film sensors
 290 [49] or polyvinylidene fluoride (PVDF) sensors [50] in the mat-
 291 tress pad, strain gauges [51], pneumatic [52], and hydraulic [53]
 292 sensors. Some researchers have also proposed the use of sensor
 293 arrays rather than single sensors to improve robustness [54],
 294 [55]. As these sensors can usually provide the additional infor-
 295 mation on respiration and body movement as well as heart beats,
 296 this information can be incorporated with the BCG to generate

sleep evaluating parameters more accurately, as well as other applications such as early warning in the general ward, or home monitoring, where rhythm and dynamics can be monitored over extended periods of time for predictive analytics.

Sleep stages have mainly been classified into two levels slow wave sleep or non-slow wave sleep (SWS/non-SWS), or three levels (wake/REM/NREM) based on BCG. The earliest implementation of BCG based sleep staging was by Watanabe and Watanabe [56]. Two stage classification between SWS and non-SWS was performed based on BCG with movement measured unobtrusively by a load cell installed bed [44]. Based on calculated heart rate variability (HRV) parameters, they achieved the mean agreement of 92.5% (kappa index of 0.62). Sleep efficiency was evaluated by detecting nocturnal awakening epochs in BCG measured using PVDF sensors on bed mattress [57], based on the principle that awakening during sleep is related with subtle changes in heart rate; thus, awakening epochs can be detected based on HRV parameters. They achieved the classification accuracy of 97.4% (kappa index of 0.83) and 96.5% (kappa index of 0.81) and evaluated the sleep efficiency with absolute error of 1.08% and 1.44% for normal subjects and obstructive sleep apnea patients, respectively.

Three stage classification (Wake/REM/NREM) of sleep has been derived using the analyses of spectral components of the heartbeats extracted from multichannel BCG based on EMFi sensors [58]. By applying a hidden Markov model only on BCG, they achieved a total accuracy of 79% (kappa index of 0.43) compared to clinical sleep staging from PSG. The performance was enhanced by combining the time variant-autoregressive model (TVAM) and wavelet discrete transform (WDT) with the quadratic (QD) or linear discriminant (LD) analysis [59]. The QD-TVAM algorithm achieved a total accuracy of 76.8% (kappa index of 0.55), while LD-WDT achieved a total accuracy of 79% (kappa index of 0.51). Although there was also a study done for sleep stage classification into four levels (wake/REM/deep sleep/light sleep) with ECG [60], four-level sleep stage classification with BCG is not reported yet. With the ECG signal, Tanida *et al.* classified the sleep stage with HRV analyzed for each 60-s epoch of ECG and calculated at three frequency band powers. Their results for minute-by minute agreement rate ranged from 32% to 72% with an average of 56% for ten healthy women.

Sleep monitoring based on BCG technology has a potential to provide both continuous and longitudinal information on a subjects' sleep quality and may take a role as a predictive screening method prior to the sleep studies based on PSG. It could also fill the gap among PSG of whole night examination and portable ambulatory PSG, which can be applied at home and simplified with, for example, a wrist worn movement sensor.

D. Chair-Based BCG and SCG systems

Chair-based systems have mainly used electromechanical film (EMFi) sensors based on piezoelectric transduction. Koivisto *et al.* attached EMFi sensors to a chair to measure BCG signals from two seated subjects, and found the signal shape to be similar to other BCG measurements from the literature

[61]. Walter *et al.* placed an EMFi mat in the cushion of the driver's seat in a car to measure the BCG for automatically monitoring driver fitness [62]. These systems provide a means for measuring BCG or SCG signals from patients who cannot stand still on their own, minimize motion artifacts, and allow the user to be comfortable during the measurement. The main disadvantages for chair-based BCG recording are the reduction of signal amplitude compared to measurements using table, bed, or weighing scale systems, and the effects of postural changes on signal quality.

IV. SIGNAL PROCESSING AND MODELING

A. Heartbeat Detection

Since heart rate is regulated by the autonomic nervous system, the analysis of HRV is currently employed to obtain physiological and clinical information on the level of sympathetic and parasympathetic drive to the heart. Even though ECG is the most widely used biological signal to evaluate heart rate dynamics, BCG may also be used. Due to its easier application for monitoring in contrast to the inconvenience of attaching electrodes to the skin in ECG measurement, BCG may facilitate the assessment of heart rate dynamics in daily life [63].

Heartbeats may be identified by the J-wave peak in the BCG signal, i.e., the point of highest amplitude in the BCG waveform. Heart rate is evaluated by measuring the interval between consecutive J-peaks, the J-J interval. As there are many algorithms to detect the R-peak in ECG, there are also various methods to detect the J-peaks or heart beat from BCG. Since BCG can be measured in different settings with different type of sensors, the peak-detection algorithm should be selected to optimize the performance considering the characteristics of measured BCG. A heartbeat detection algorithm which showed high performance in R-peak detection from ECG can be applied with minor modification for J-peak detection. Generally the peak detection procedure is applied to select the highest value in amplitude as the J-peak within the sliding window after some preprocessing to increase signal-to-noise ratio (SNR) and to reject artifacts due to motion or other interferences.

Choi *et al.* demonstrated increased detection performance with a dedicated algorithm, which finds local peaks in four divided subintervals within a period and selects the maximum peak as J-peak from these local peaks with some rejection rules [44]. Jansen *et al.* applied a detection method based on a "template matching" rule by evaluating a correlation function in a local moving window [64], a method which was further refined and developed by Shin *et al.* [65]. Although this method requires template design in its first stage, Shin *et al.* successfully applied it to several types of BCG signals acquired from air mattress, load cells, and EMFi sensors. The results showed 95.2% of sensitivity and 94.8% of specificity in average for five subjects and three types of BCG signals. Additional methods for heartbeat detection from BCG signals include those which combine different estimators [46], [66], [67], and methods which use wavelets to preprocess the signal prior to peak detection [53], [68].

Heart rate was estimated from the spectral domain specially focusing on third harmonics especially in BCG signals acquired

with fiber optic sensors [45]. The results showed an error less than 0.34 beat/min in 2°min averaged heart rate. Heartbeat intervals were calculated with the cepstrum method, by applying FFT for short time windows including pair of consequent heart beats [48]. Relative error of the method was 0.35% for 15 night recordings with six normal subjects after rejecting movement artifacts. Since the results of heart beat detection are not perfect, generally visual editing is required to correct the errors in peak detection for further application like HRV analysis. Multi-channel fusion techniques have also been demonstrated recently for BCG-based heartbeat detection [48], [69].

Recently, Paalasmaa *et al.* [70] and Brueser *et al.* [71] both verified heartbeat detection algorithms on large datasets containing hundreds of thousands of heartbeats recorded in uncontrolled environments. Paalasmaa *et al.* used hierarchical clustering to first infer a heartbeat shape from the recordings, then beat-to-beat intervals were found by determining positions at which this template best fit the signal. The mean beat-to-beat interval error was 13 ms from 46 subjects in the clinic, home, single bed, double bed, and with two sensor types. Brueser *et al.* demonstrated robust estimation of heartbeats for 33 subjects of which 25 were insomniacs, with a mean beat-to-beat interval error of 0.78%. Their method used three short-time estimators combined using a Bayesian approach to continuously estimate interbeat intervals. Automatic template learning approaches were also presented by Brueser *et al.* in 2011 with low error [51].

Performance of HRV analysis using BCG measured on weighing scale-type load cell is evaluated in reference to the ECG during the resting and under each condition of Valsalva and postexercise sessions that induce cardiac autonomic rhythm changes [72]. Time domain, frequency domain, and nonlinear domain HRV parameters were evaluated on 15 healthy subjects to assess the cardiac autonomic modulation under each of these conditions. For all subjects and for all experimental sessions, HRV parameters calculated from BCG peak intervals are statistically not different from those obtained from the reference ECG. The results showed high performance with relative errors of 5.0–6.0% and strong correlation of 0.97–0.98 in average for these three states compared with the results from ECG peaks. The errors were relatively high in HRV parameters reflecting the high-frequency characteristics of heart rates such as HF, LF/HF in the spectral analysis, pNN50 in time-domain analysis, and SD1 in nonlinear analysis. This is considered to be caused by the inaccuracy in detecting peak from the less sharp J-peak of BCG compared to the R-peak in ECG. HRV estimates with BCG have also been compared to the PPG, and the correlation between the two was found to be high [73]. Preliminary work was recently presented by Brueser *et al.* for unsupervised HRV estimation from BCG signals [74].

B. Noise and Interference Reduction

Several sources of noise and interference can potentially corrupt BCG and SCG measurements taken using modern systems. These include sensor and circuit noise [75], motion artifacts [15], [21], [76], [77], and floor vibrations (for standing BCG measurements) [78].

Both BCG and SCG represent low-level signals that contain very low-frequency information—this can lead to problems with flicker (1/f) noise in the sensor interface circuit corrupting the measurements. Furthermore, many diseased subjects, and elderly subjects, have smaller signal amplitudes compared to the healthy young population [79]. The sensor and circuit noise were characterized and reduced for weighing-scale-based BCG systems using an ac-bridge amplifier approach [75]. This approach led to a SNR improvement of 6 dB.

For ambulatory and standing subjects, motion artifacts present the greatest potential obstacle to achieving reliable measurements. Unlike bed or chair systems, where the subject stays generally still for the measurement, postural sway, or ambulation can create unwanted peaks or distortion in the measured signals. Motion artifact detection for standing BCG measurements was accomplished using auxiliary sensors as noise references; then, gating the BCG signal based on the detection of excessive noise [76], [80]. In one study, the noise reference was an extra strain gauge added to the scale to detect postural sway [76]. In another study, the rms power of the electromyogram signal from the feet, indicating the presence of increased muscle contractions due to excessive movement, was used as a noise gate for the BCG [80]. Pandia *et al.* presented preliminary methods for cancelling motion artifacts in SCG signals from walking subjects, improving overall heartbeat detection [77]. Di Rienzo *et al.* used an automatic selection of movement-free data segments from daily recordings of SCG signals from ambulant subjects, followed by an ECG triggered ensemble averaging to reduce signal noise [21]. This enabled, for the first time, the assessment of systolic time interval profiles during normal daily living.

BCG measurements taken in a direction orthogonal to the plane of the floor can potentially be corrupted by floor vibrations—this can particularly pose a challenge for measurements taken on a vehicle [62] or plane [81]. Walter *et al.* instrumented the seat of a car with an EMFi mat to measure the BCG, aiming to use the information to monitor driver fitness [62]. However, with the engine turned on, the BCG was corrupted by vibration artifacts and rendered unusable. Inan *et al.* used an auxiliary sensor for vibration detection and adaptive noise cancellation to cancel floor vibration artifacts in the BCG measurement [78]. In this study, high-quality BCG measurements were successfully demonstrated from a subject standing on a bus with the engine turned on and idling. Additionally, it was observed that low-noise SCG waveforms could be obtained in a subject sitting in the metro, while a train was going by, with the above mentioned ensemble averaging approach [21].

C. Signal Modeling

Modeling of SCG and BCG provides a tool to better understand the genesis of waves in these signals and to simulate their morphological changes with different myocardial abnormalities. Modeling of BCG goes back to the early years of ballistocardiographic research [79].

In most BCG recording systems, the recording device is quite small compared to the human body and the platform on which it rests. It is also far away from the heart in most cases; thus,

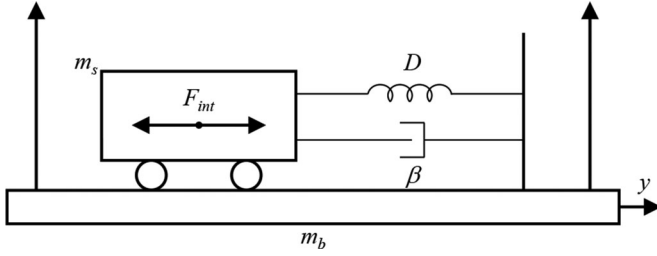


Fig. 3. Schematic showing the subject (with mass, m_s) and the BCG recording system (with mass, m_b) coupled by a spring dashpot system.

TABLE II
DESCRIPTIONS OF VARIABLES FOR SIGNAL MODELING

Variable	Description
F_{int}	Internal forces
β	Damping constant
y	Displacement or (in subscript) indicating head-to-foot direction
\dot{y}	Velocity
\ddot{y}	Acceleration
D	Spring constant
m_s	Mass of subject
m_b	Mass of recording device

the volume of the heart has been neglected in such models. The heart has been modeled like a point source providing the flow to the circulation system model [82]. Such a model is in accordance with the classical definition of BCG to be resulted through movement of center of gravity of the body and platform. On the contrary, in SCG the recording device (i.e., accelerometer) is near the heart and the volume of the heart cannot be neglected in any model dealing with SCG or any other precordial vibration signal. Thus, except for some preliminary efforts [83] SCG modeling has not been pursued by many researchers, probably because of the complications associated with such a model.

In ballistocardiographic research, one can study the events within human body that cause its movement in space, regardless of the recording device or to study the properties of instruments recording them and how their record relates to the movement originating them. Both of these two approaches are briefly introduced.

1) *Modeling the Recording Device:* During the early years of ballistocardiographic research, several different instruments were used to measure BCGs, from beds hanging from the ceiling [84] to tables strongly coupled to ground [1]. These instruments were giving different records from the same normal subjects. So, efforts were made to model the effect of these instruments on BCG morphology. Limiting ourselves to the head-foot direction the equation giving the components along the y -axis (Fig. 3, variables defined in Table II) reads:

$$(F_{int})_y - \beta\dot{y} - Dy = (m_s + m_b)\ddot{y}. \quad (1)$$

After sorting and substituting $(F_{int})_y$ into $m_s\ddot{y}_c$ (where \ddot{y}_c is the acceleration of center of mass of body):

$$(m_s + m_b)\ddot{y} + \beta\dot{y} + Dy = m_s\ddot{y}_c. \quad (2)$$

From the above equation, three different classic types of BCGs can be conceived based on the fact that which terms on the left side of the above equation can be neglected. The first is

$$(m_s + m_b)\ddot{y} = m_s\ddot{y}_c \quad (3)$$

which means that the movement of bed and body is proportional to the movement of the center of gravity. A good approximation of this special case is when the ballistocardiograph is weakly coupled to the environment such as ultralow frequency BCG (ULF-BCG) systems.

The second type is when:

$$\dot{y} = \frac{m_s}{\beta}\ddot{y}_c \quad (4)$$

which represents Nickerson's low-frequency (LF) BCG and the third type is when:

$$y = \frac{m_s + m_b}{\beta}\ddot{y}_c \quad (5)$$

which refers to the situation when BCG is strongly coupled to its environment, which were categorized under high-frequency BCG (HF-BCG). In other words, when the resonance frequency of the BCG platform is much higher than heart frequency, then its displacement is proportional to the internal acceleration of body's center of gravity.

From this theoretical evaluation, it is clear that very different results will be obtained when one records any one aspect of motion such as displacement or acceleration from each of the three ideal types of ballistocardiographs [82]. However, there is a fourth category of classical BCGs, which are the direct body recordings based on AHA consensus paper on BCG terminology [85]. Direct body BCGs were always criticized for their inconsistencies [82].

2) *Modeling the Internal Forces:* Starr started on BCG modeling, where arteries were segmented into 3-cm long pieces and mass of blood in the aortic segment closest to the aortic valve was multiplied by acceleration, derived from cardiac ejection curve, to calculate force. This was repeated when the blood volume shifted to the next segment [82].

A more comprehensive model of human systemic arterial tree with distributed properties was constructed in early 1960s by Starr and Noordergraaf [82] and was improved later on by Westerhof *et al.* [86]. This model was based on the fact that, when using ULF systems, in which the body was free to move in space in the head-foot axis, it was observed that the body moved first footward and then headward during the cardiac cycle. This was explained as a movement to counteract the displacement of the blood mass, that, shortly after the onset of systole, is first driven headward out of the heart to distend the great vessels, and later footward, as the pulse wave spreads peripherally and blood accumulates at a great distance from the heart in the more peripheral vessels.

The model divided the arterial tree in 115 segments and calculated the position of the body's center of gravity in the longitudinal direction $y_c(t)$, as a function of time, by numerical integration of the products of the excess masses of each segment during the interval t , and the distance y_i between the centre of

each segment and the reference plane. Noordergraaf's model was successful in quantitatively predicting the amplitudes of ULF BCG waves and in giving an explanation for the origin of the main peaks. The model was verified on the data acquired from an astronaut in MIR station [87], where by using the longitudinal BCG recorded in space the model could be used to derive the aortic flow.

V. HUMAN SUBJECTS STUDIES WITH MODERN SYSTEMS

A. Correlation Studies With Healthy Subjects

Originally, BCG and SCG were proposed as diagnostic tools for the clinic—for example, a patient would lie on a Starr BCG table, the recording would be printed on a strip chart, and the physician would read the recording to make a diagnosis regarding the patient's cardiovascular health [1], [5]. However, the large intersubject variability in the signals hampered this approach, particularly given the limited tools available at that time for signal analysis. On the contrary, studies have shown that the intrasubject variability in the signals over serial measurements is actually low [15]—except in the presence of changing cardiovascular health. For this reason, in the past decade the BCG and SCG have been proposed as tools for monitoring changes in the same patient's health overtime. Then, the subject is his/her own control, and intersubject variability is no longer an obstacle.

To uncover the clinical relevance of BCG and SCG signal features, and to pave the way for future studies with clinical populations, several researchers conducted human subjects studies with a healthy population using modern instrumentation and analysis tools. These studies were mainly designed with a noninvasive protocol for altering the hemodynamics and timing intervals of the heart—such as exercise, Valsalva maneuver, whole-body tilt testing, or lower body negative pressure (LBNP)—then, comparing the changes in the BCG or SCG waveform to changes in a reference standard measurement, such as impedance cardiography (ICG) or Doppler ultrasound.

For both BCG and SCG signals the amplitude (or rms power) components have been shown to modulate with changes in left ventricular function—in particular, changes in stroke volume (SV) or cardiac output (CO). Castiglioni *et al.* measured clavicular SCG signals before and immediately after exercise and compared the percent changes in the peak-to-peak amplitude of the SCG to changes in CO as measured by the finometer model flow method, finding a strong correlation for four data points taken from four subjects [24]. Inan *et al.* further demonstrated that the changes in rms power resulting from exercise, measured during 10 min of recovery time, were strongly correlated to changes in CO measured by Doppler ultrasound for 275 data points taken from nine subjects [88]. Tavakolian *et al.* trained a neural network to estimate SV from SCG parameters and tested this classifier on a separate testing dataset, finding an average correlation coefficient of 0.61, and Bland–Altman agreement limits (95% confidence) of +7.4mL, −7.6mL for 4900 heartbeats analyzed from eight participants [16]. It is important to note that these error bands are larger than what would be needed for absolute volume estimation using the SCG; however, this may be of interest for future research.

Many researchers have also examined the time intervals both within the signals themselves, and between BCG / SCG signal features and other physiological measurements (e.g., ECG or PPG), to form a relationship between these timing intervals to more well-known parameters [e.g., preejection period (PEP), pulse transit time (PTT), or left ventricular ejection time (LVET)]. The time interval between the ECG R-wave peak and the BCG J-wave peak has been proposed as a surrogate for the PEP—a measure of the IVC period of the heart and an index of cardiac contractility [30], [89]. These authors used the Valsalva maneuver and/or whole body tilt testing to modulate the PEP by changing the autonomic balance between parasympathetic and sympathetic drive, and compared the R-J interval to the PEP measured using ICG. Etemadi *et al.* demonstrated a strong correlation ($R^2 = 0.86$) between the R-J interval and the PEP for 2126 heartbeats across ten subjects performing the Valsalva maneuver [89]. He *et al.* showed similar results for one example subject with both the Valsalva maneuver and whole-body tilt testing [30]. Tavakolian *et al.* proposed the interval between the ECG Q-wave and the SCG AO-point as a surrogate for PEP, and found strong correlation between this interval and PEP measurement using ICG and Doppler ultrasound in 25 subjects [16].

Researchers have also attempted to extract data from the BCG relating to blood pressure (BP), leveraging the known relationship between pulse wave velocity estimated using PTT, and Pinheiro *et al.* suggested the use of BCG and PPG for PTT estimation [90]. Shin *et al.* compared the R-J interval of the BCG, modulated using the Valsalva maneuver, to beat-by-beat systolic BP (SBP) measurements taken using the Finapres system, finding a strong correlation [39]. Nevertheless, Casanella *et al.* found that, in case of hemodynamic changes induced by paced respiration, this correlation between R-J interval and SBP was dependent on the subject and was not always observed [91]. Winokur *et al.* found, for one example subject, that the time interval between the BCG and the PPG signal, both measured at the ear, were correlated to PTT, and could thus be used to estimate BP [31].

Another important interval is the duration of systolic ejection, the LVET, as it provides an indication of what percentage of the cardiac cycle is being devoted to ejection compared to filling. Tavakolian *et al.* used LBNP to simulate hemorrhage, and found that LVET measurements taken using SCG were significantly different at various stages of LBNP, and correlates with the LBNP levels ($R = 0.90$) for 32 subjects [92]. Di Rienzo *et al.* found that with exercise LVET changes measured using wearable SCG are in line with the changes reported in the literature and obtained by traditional laboratory techniques [21], [93].

B. Clinical Findings From Patients With Cardiovascular Disease

Modern ballistocardiography and seismocardiography systems may be capable of monitoring slow, longitudinal changes in cardiac function associated with a number of cardiovascular diseases. Timely noninvasive detection of subtle changes in cardiac pathophysiology may one day enable daily drug dosage adjustments, thus reducing costly and morbid rehospitalizations

[94]. At this moment, the feasibility of this approach is investigated by the ongoing LAPTOP-HF study which, however, uses an implantable right atrial pressure sensor coupled to a mobile device that allows daily automatic dosage adjustment [95].

Fortunately, the basis for the SCG's clinical utility was begun in 1990 with the initial use of high sensitivity, LF accelerometers to measure precordial vibrations [96]. Significant features of the SCG waveform were identified and associated with key events in the cardiac cycle [17]. This allowed the accurate measurement of these features (e.g., ACs and MOs) using one sensor, greatly simplifying the calculation of CTIs.

A large body of work exists on the utility and efficacy of CTIs [97], [98]. This knowledge combined with the ability to make accurate, repeatable quantitative measurements using the SCG resulted in the ability to conduct clinically relevant cross-sectional studies. Subsequently, clinical studies were undertaken to determine if the SCG could be used to identify changes in the SCG waveform resulting from myocardial ischemia [99].

The SCG's clinical utility in enhancing the diagnostic outcome of a graded exercise stress test was first shown in [100]. A large multicenter study demonstrated that when the combined results of the ECG and SCG were used, the predictive accuracy of detecting physiologically significant coronary artery disease was increased significantly over the results of the ECG alone [7].

The introduction in the early 1990s of lightweight (<25g) accelerometers, whose working range extended below 1 Hz, made possible other clinical settings for the SCG. The SCG as a magnetic-field-compatible alternative to the electrocardiogram for cardiac stress monitoring [101] was made possible using a newly introduced light weight piezoelectric accelerometer (336C, PCB Piezotronics, Depew, NY, USA).

The SCG was used to measure CTI's during atrial, ventricular, and biventricular pacing, as compared to normals [102]. One of the studies objectives was to determine the utility of the SCG in cardiac resynchronization therapy (CRT). This study was the first to use 3 SCG traces for analysis, i.e., one accelerometer was placed on the xiphoid process, a second over the apex at the fourth intercostal, and a third on the right carotid pulse.

In 1994, the SCG was used to make accurate longitudinal measurements in a study of the effects of elgodipine on cardiac hemodynamics [103]. In a sports medicine application, exercise capacity was evaluated using the SCG [104]. A more extensive review of the SCG is available in [105].

As a note of interest, the combined patient population of the myocardial ischemia studies [7], [100] is close to 2000 and consists of both healthy and disease subjects. All the raw data were recorded with the same instrumentation (SCG 2000, SeisMed Instruments, Minneapolis, MN, USA) associated with these datasets are complete patient demographics. A project is underway to make the raw data available on the PhysioNet website for study by interested researchers [105].

More recent findings with BCG and SCG further support that the signals have great potential in allowing proactive cardiac disease management without a costly implantable device. However, despite stated clinical and/or physiologic motivations, the overwhelming majority of modern BCG/SCG findings continue to be from healthy subjects [106]–[108]. Notable exceptions in-

clude a bed-mounted BCG system for automated detection of atrial fibrillation [109], the observation of reduced signal amplitude in the setting of premature atrial or ventricular contractions [15], and the reduction of signal consistency in heart failure patients concordant with worsening clinical outcome [110].

One particular subset of patients is particularly well suited for study using cardiomechanical signals, those undergoing CRT. CRT patients have abnormal cardiac conduction causing in a significant delay between the pumping action of the various chambers of the heart. CRT involves precisely adjusting the timing of a multichamber pacemaker to reduce or remove these delays. Such timing is difficult to ascertain using available technologies, spawning the field of "CRT optimization." Researchers recently demonstrated the benefits of intracardiac acceleration monitoring in performing CRT optimization [111], a finding preliminarily corroborated by BCG findings as well [8].

C. 3-D Ballistocardiography and Microgravity Studies

As the sections on instrumentation earlier in this review have indicated, measurements of BCG (in particular) are constrained by the coupling of the body to the ground, a direct result of the influence of gravity. As such, full 3-D recordings of the BCG are difficult in the terrestrial environment, and much of the focus has been on accelerations in the coronal plane (the XY plane as defined in the section on measurement axes).

Given this limitation, it is therefore not surprising that the idea of measuring the BCG in a subject in free-fall (weightlessness, zero-G, microgravity) was an obvious target of investigation. The first such experiment was performed in the 1960s in parabolic flight, with the subject strapped into a "tub," which was itself instrumented to record the BCG [9]. Despite the limited periods of microgravity available (typically ~20 s) and the subject restraints, recordings of good quality were obtained.

Spaceflight represents the other obvious environment in which the "true" 3-D BCG can be recorded. The earliest recordings were made by the Soviets on Saluyt-6 [10] and consisted of a series of five recordings were performed in two crew members of a long duration mission on days 46, 71, 98, 133, and 175. A piezoelectric sensor, attached close to the center of mass, recorded ballistic forces in the feet-to-head axis during breath holding experiments. Individual changes were seen during the mission with maximum amplitude of the IJ wave occurring on day 133. Measurements were also made during the Spacelab-1 mission aboard the Space Shuttle in 1983 [112]. These experiments were conducted in two subjects at two occasions during this short duration spaceflight and showed an increase of the overall systolic accelerations along the longitudinal axis in microgravity.

Perhaps the best-analyzed dataset of the BCG in spaceflight came from measurements made during the Spacelab D-2 mission in 1993. During that flight, extra time became available (due to an extension of the overall mission length), and an experiment was hastily conceived, approved, implemented, and performed to measure 3-D BCG in a free-floating subject. Parenthetically, this may be one of the fastest spaceflight experiments ever developed with the time from concept, to collection of the data



Fig. 4. Subject in D-2 shown wearing the snugly-fitting suit incorporating a respiratory inductance plethysmograph and ECG. Photo Credit: NASA.

816 (including approval of an institutional review board) was only
 817 4–5 days, surely some sort of record. The experiment utilized
 818 data from a free-floating subject instrumented with an ECG
 819 and wearing a snugly fitting suit that measured respiratory
 820 motion using an impedance plethysmograph (see Fig. 4). This
 821 instrumentation was a part of the Anthrock series of human
 822 studies managed by the European Space Agency. The second
 823 crucial piece of instrumentation was a set of high-fidelity tri-
 824 axial accelerometer that were attached to the vehicle and used
 825 for measuring the accelerations imparted by crew activity in
 826 the Spacelab. The sensor package was detached from the ve-
 827 hicle and taped to the lumbar region of the subject, near to
 828 the (presumed) center of mass. Data were then recorded as
 829 the subject remained stationary and free floated in the center
 830 of the Spacelab, providing a continuous recording, free of in-
 831 terruptions of 146 s. In order to synchronize the two separate
 832 data streams, collisions with the Spacelab structure, which dis-
 833 rupted signals in both data streams, were used as posthoc event
 834 source [11].

835 The data from the D-2 study and some subsequent studies
 836 provided valuable insight into several aspects of the BCG. In
 837 particular there were four major conclusions derived from this
 838 dataset.

- 839 1) Lung volume greatly influences the accelerations
 840 recorded, especially in the longitudinal (head-to-foot)
 841 body axis (see Fig. 5), with the implication being that
 842 there is better coupling between the heart and the body in
 843 the longitudinal axis at higher lung volumes [11]. Inter-
 844 estingly, the actual direction of respiratory motion (mid
 845 inspiration versus mid expiration) had only minimal in-
 846 fluence of the BCG.
- 847 2) Data derived from short periods of microgravity in
 848 parabolic flight are largely equivalent to data obtained
 849 in sustained microgravity [113].
- 850 3) The BCG has a plane of symmetry that is primarily sagi-
 851 tal. This suggests that 2-D recordings performed in a
 852 supine subject (i.e., coronal recordings) fail to capture
 853 a significant portion of the effect of the blood ejection on
 854 the body, complicating their interpretation [113].

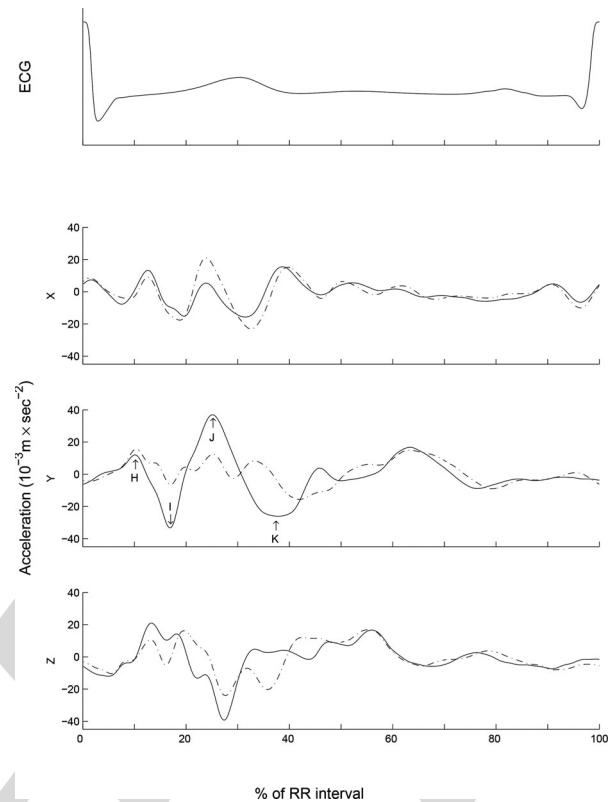


Fig. 5. The 3-D BCG recorded in spaceflight in a free-floating subject, at the end of a normal expiration (dashed lines, functional residual capacity, FRC), and at the end of a normal inspiration (solid lines, FRC + tidal volume). From [11].

- 4) The accelerations that are recording in a 2-D system are only modestly correlated with the true 3-D accelerations that actually occur, again complicating their interpretation [113].

BCG flight experiments were also an integral part of the Russian cardiovascular research program for the orbital station MIR. BCG along the head-to-foot direction was measured in three crew members during the second MIR mission in 1988 and compared to SCG recordings. Significant changes of the BCG amplitudes (HI, IJ, JK) during the long-term flight were described together with large inter individual differences. The first true 3-D-BCG recordings were made during the sixth MIR mission in 1990 in two crew members on flight days 56 and 110. Three new piezoelectric sensors were used placed in perpendicular planes in a small cylindrical box with a diameter of 40 mm and a height of 20 mm. The sensitivity of the sensor was 20 mV/m/s². The sensor was placed between the scapulae using rubber belts and a metallic plate. The special amplifier (BCG-3) was connected to the recording unit “Gamma-1,” and the data were transmitted telemetrically to the ground station. In summary, no dramatic changes in the vector sum were detected. Maximum forces ranged from 5.85 to 10.18 N. However, profound individual changes of the shape, amplitude, and timing of the BCG, especially in the lateral and dorso-ventral plane have been found. Finally, combined BCG and SCG measurements have been made every month in space during the 14 months space flight of Valeri Poljakov,

882 15th to 17th MIR missions (Russian–Austrian flight experiment
883 “Pulstrans”) [114].

884 VI. STANDARDS AND OPEN ISSUES

885 A. Need For a Standardization

886 From the analysis of the literature, it appears that important
887 methodological aspects concerning BCG and SCG analysis are
888 still characterized by a certain level of ambiguity. These include

889 1) *Definitions of BCG and SCG Signals*: In the literature, the
890 definition of BCG and SCG is not univocal and the “BCG” term
891 is even sometimes used for SCG signals.

892 2) *Nomenclature*: Since BCG and SCG waveforms are
893 mostly different (although they might have some common fea-
894 tures to be investigated) it is reasonable to use a specific nomen-
895 clature for defining peaks and valleys of each signal. The preva-
896 lent annotation for BCG was proposed by Starr *et al.* [1], for
897 SCG by Crow *et al.* [17]. However, there are some disagree-
898 ments on these annotations, and in some instances, SCG peaks
899 are termed with the BCG annotation.

900 3) *Indication of Site of Measurement, Characteristics of sen-
901 sor, Sensor Axis Orientation*: These pieces of information are
902 crucial for data comparison and interpretation, but unfortunately
903 are not invariably reported in scientific communications.

904 A standardization or at least a common position on the above
905 issues would greatly facilitate the understanding and comparison
906 of published results, the exchange of data, and the design of new
907 experimental protocols in this area.

908 B. Open Issues

909 A number of open issues remain to be addressed in this field to
910 improve the understanding and applicability of BCG and SCG
911 signals. Hereafter, we provide just a short list of these issues.

- 912 1) The biological meaning of BCG and SCG deflections not
913 yet annotated and their clinical relevance.
- 914 2) Possible common features of the BCG and SCG signals.
- 915 3) Further parameters derivable from the analysis of the BCG
916 and SCG 3-D vectors.
- 917 4) Effects of respiration, posture, right ventricle, and sensor
918 adherence on the signal waveform/quality.
- 919 5) How to facilitate the use of these signals in clinical prac-
920 tice?
- 921 6) Reference values for healthy and diseased subjects for
922 both types of signals, and for a wide range of body
923 types/sizes, and ages.

924 VII. CONCLUSION AND AREAS FOR FUTURE INVESTIGATION

925 The recent advances in the BCG and SCG field indicate the
926 strong potential of these measurements to address wide vari-
927 ety of clinical needs, in particular monitoring or trending the
928 cardiomechanical health of patients outside of the clinic. Both
929 BCG and SCG measurements can be taken using inexpensive
930 and unobtrusive sensors, making them ideally suited, for exam-
931 ple, for home monitoring of chronic diseases. Nevertheless, to
932 maximize our ability to interpret these signals, the physiological

origins of both signals must be studied further and elucidated. 933
Furthermore, there is a need to be able to map each measure- 934
ment modality to another using cardiovascular and mechanical 935
modeling of the body, such that any BCG or SCG waveform 936
amplitude, timing, or morphology measured using one modal- 937
ity can be translated quantitatively to another. For example, 938
if a bed-based recording in the dorso–ventral axis yielded a 939
peak BCG J-wave amplitude of 2 N, system modeling tools are 940
needed to compare this to a corresponding J-wave amplitude 941
measured using a weighing scale. Finally, an extensive, open 942
database of BCG and SCG signals, processing tools, and even 943
microprocessor code needs to be made available to massively 944
expand the capability of researchers around the world to inves- 945
tigate these signals, use them in their own settings, and grow the 946
field from a niche into an established technique, routinely used 947
in clinical practice. 948

REFERENCES 949

- [1] I. Starr, A. J. Rawson, H. A. Schroeder *et al.*, “Studies on the estimation 950
of cardiac output in man, and of abnormalities in cardiac function, from 951
the heart’s recoil and the blood’s impacts; the ballistocardiogram,” *Amer.* 952
J. Physiol., vol. 127, pp. 1–28, 1939. 953
- [2] B. S. Bozhenko, “Seismocardiography—a new method in the study 954
of functional conditions of the heart [Article in Russian],” *Ter Arkh.* 955
vol. 33, pp. 55–64, 1961. 956
- [3] J. W. Gordon, “Certain molar movements of the human body produced 957
by the circulation of the blood,” *J. Anat. Physiol.*, vol. 11, pp. 533–536, 958
1877. 959
- [4] D. M. Salerno and J. Zanetti, “Seismocardiography for monitoring 960
changes in left ventricular function during ischemia,” *Chest J.*, vol. 100, 961
pp. 991–993, 1991. 962
- [5] I. Starr and F. C. Wood, “Studies with the ballistocardiograph in acute 963
cardiac infarction and chronic angina pectoris,” *Amer. Heart J.*, vol. 25, 964
pp. 81–101, 1943. 965
- [6] H. Mandelbaum and R. A. Mandelbaum, “Studies utilizing the portable 966
electromagnetic ballistocardiograph: IV. The clinical significance of se- 967
rial ballistocardiograms following acute myocardial infarction,” *Circu-* 968
lation, vol. 7, pp. 910–915, 1953. 969
- [7] R. A. Wilson, V. S. Bamrah, J. J. Lindsay *et al.*, “Diagnostic accu- 970
racy of seismocardiography compared with electrocardiography for the 971
anatomic and physiologic diagnosis of coronary artery disease during 972
exercise testing,” *Amer. J. Cardiol.*, vol. 71, pp. 536–545, 1993. 973
- [8] L. Giovangrandi, O. T. Inan, R. M. Wiard *et al.*, “Ballistocardiography: 974
A method worth revisiting,” in *Proc. IEEE Annu. Int. Conf. Eng. Med.* 975
Biol. Soc., 2011, pp. 4279–4282. 976
- [9] W. C. Hixson and D. E. Beischer, “Biotelemetry of the triaxial ballisto- 977
cardiogram and electrocardiogram in a weightless environment,” *Naval* 978
School Aviat. Med., Pensacola, FL, USA, 1964. 979
- [10] R. M. Baevsky and I. I. Funtova, “Ballistocardiographic examinations of 980
the salyut-6 fourth expedition crew members,” *Komsich Biologiya Aviak* 981
Medit, vol. 16, pp. 34–37, 1982. 982
- [11] G. K. Prisk, S. Verhaeghe, D. Padeken *et al.*, “Three-dimensional ballis- 983
tocardiography and respiratory motion in sustained microgravity,” *Aviat.* 984
Space Environ. Med., vol. 72, pp. 1067–1074, 2001. 985
- [12] P. F. Migeotte, S. De Ridder, J. Tank *et al.*, “Three dimensional ballisto- 986
and seismo-cardiography: HIJ wave amplitudes are poorly correlated to 987
maximal systolic force vector,” in *Proc. IEEE Annu. Int. Conf. Eng. Med.* 988
Biol. Soc., 2012, pp. 5046–5049. 989
- [13] R. M. Wiard, H. J. Kim, C. A. Figueroa *et al.*, “Estimation of central aortic 990
forces in the ballistocardiogram under rest and exercise conditions,” in 991
Proc. IEEE Annu. Int. Conf. Eng. Med. Biol. Soc., 2009, pp. 2831–2834. 992
- [14] M. Di Rienzo, P. Meriggi, F. Rizzo *et al.*, “A wearable system for the 993
seismocardiogram assessment in daily life conditions,” in *Proc. IEEE* 994
Annu. Int. Conf. Eng. Med. Biol. Soc., 2011, pp. 4263–4266. 995
- [15] O. T. Inan, M. Etemadi, R. M. Wiard *et al.*, “Robust ballistocardiogram 996
acquisition for home monitoring,” *Physiol. Meas.*, vol. 30, pp. 169–185, 997
2009. 998

- 999 [16] K. Tavakolian, "Characterization and analysis of seismocardiogram for
1000 estimation of hemodynamic parameters," Ph.D. dissertation, Dept. Appl.
1001 Sci, School Eng. Sci., Simon Fraser Univ., Burnaby, BC, Canada, 2010.
- 1002 [17] R. S. Crow, P. Hannan, D. Jacobs *et al.*, "Relationship between seismo-
1003 cardiogram and echocardiogram for the events in the cardiac cycle,"
1004 *Amer. J. Noninvasive Cardiol.*, vol. 8, pp. 39–46, 1994.
- 1005 [18] O. T. Inan, M. Etemadi, R. M. Wiard *et al.*, "Novel methods for esti-
1006 mating the ballistocardiogram signal using a simultaneously acquired
1007 electrocardiogram," in *Proc. IEEE Annu. Int. Conf. Eng. Med. Biol. Soc.*,
1008 2009, pp. 5334–5347.
- 1009 [19] K. Pandia, O. T. Inan, G. T. A. Kovacs *et al.*, "Extracting respiratory
1010 information from seismocardiogram signals acquired on the chest using a
1011 miniature accelerometer," *Physiol. Meas.*, vol. 33, pp. 1643–1660, 2012.
- 1012 [20] Y. Chuo and B. Kaminska, "Sensor layer of a multiparameter single-point
1013 integrated system," *IEEE Trans. Biomed. Circuits Syst.*, vol. 3, no. 4,
1014 pp. 229–240, Aug. 2009.
- 1015 [21] M. D. Rienzo, E. Vaini, P. Castiglioni *et al.*, "Wearable seismocardiogra-
1016 phy: Towards a beat-by-beat assessment of cardiac mechanics in ambu-
1017 lant subjects," *Autonomic Neurosci.*, vol. 178, pp. 50–59, 2013.
- 1018 [22] B. Ngai, K. Tavakolian, A. Akhbardeh *et al.*, "Comparative analysis
1019 of seismocardiogram waves with the ultra-low frequency ballistocardi-
1020 ogram," in *Proc. IEEE Annu. Int. Conf. Eng. Med. Biol. Soc.*, 2009,
1021 pp. 2851–2854.
- 1022 [23] M. J. T. Paukkunen, M. T. Linnavuo, and R. E. Sepponen, "A portable
1023 measurement system for the superior-inferior axis of the seismocardi-
1024 ogram," *J. Bioeng. Biomed. Sci.*, vol. 3, 2013.
- 1025 [24] P. Castiglioni, A. Faini, G. Parati *et al.*, "Wearable seismocardiography,"
1026 in *Proc. IEEE 29th Annu. Int. Conf. Eng. Med. Biol. Soc.*, 2007, pp. 3954–
1027 3957.
- 1028 [25] Y. Chuo, M. Marzencki, B. Hung *et al.*, "Mechanically flexible wireless
1029 multisensor platform for human physical activity and vitals monitoring,"
1030 *IEEE Trans. Biomed. Circuits Syst.*, vol. 4, no. 5, pp. 281–294, Oct. 2010.
- 1031 [26] R. M. Baevsky, I. I. Funtova, A. Diedrich *et al.*, "Autonomic function
1032 testing aboard the ISS using 'PNEUMOCARD'," *Acta Astronautica*, vol.
1033 65, pp. 930–932, 2009.
- 1034 [27] P. F. Migeotte, Q. Deliere, J. Tank *et al.*, "3D-ballistocardiography in
1035 microgravity: Comparison with ground based recordings," presented at the
1036 *IEEE Eng. Med. Biol. Soc.*, Osaka, Japan, 2013, pp. 7012–7016.
- 1037 [28] E. Luchitskaya, Q. Deliere, A. Diedrich *et al.*, "Timing and source of the
1038 maximum of the transthoracic impedance cardiogram (dZ/dt) in relation
1039 to the H-I-J complex of the longitudinal ballistocardiogram under gravity
1040 and microgravity conditions," presented at the *IEEE Eng. Med. Biol. Soc.*,
1041 Osaka, Japan, 2013, pp. 7294–7297.
- 1042 [29] Q. Deliere, P. F. Migeotte, X. Neyt *et al.*, "Cardiovascular changes in
1043 parabolic flights assessed by ballistocardiography," presented at the *IEEE
1044 Eng. Med. Biol. Soc.*, Osaka, Japan, 2013, pp. 3801–3804.
- 1045 [30] D. D. He, E. S. Winokur, and C. G. Sodini, "A continuous, wearable, and
1046 wireless heart monitor using head ballistocardiogram (BCG) and head
1047 electrocardiogram (ECG)," in *Proc. IEEE Annu. Int. Conf. Eng. Med.
1048 Biol. Soc.*, 2011, pp. 4729–4732.
- 1049 [31] E. S. Winokur, D. D. He, and C. G. Sodini, "A wearable vital signs
1050 monitor at the ear for continuous heart rate and pulse transit time mea-
1051 surements," in *Proc. IEEE Annu. Int. Conf. Eng. Med. Biol. Soc.*, 2012,
1052 pp. 2724–2727.
- 1053 [32] E. Hyun, S. Noh, C. Yoon *et al.*, "Patch type integrated sensor system
1054 for measuring electrical and mechanical cardiac activities," presented
1055 at the *IEEE Sensors Applications Symposium (SAS)*, Queenstown, New
1056 Zealand, 2014.
- 1057 [33] G. Balakrishnan, F. Durand, and J. Guttag, "Detecting pulse from head
1058 motions in video," in *Proc. IEEE Conf. Comput. Vis. Pattern Recog.*,
1059 2013, pp. 3430–3437.
- 1060 [34] J. Williams. 1990, *Bridge Circuits: Marrying Gain and Balance. Linear
1061 Technology Application Note 43.*
- 1062 [35] S. I. Chaudhry, J. A. Mattera, J. P. Curtis, *et al.*, "Telemonitoring in
1063 patients with heart failure," *N. Engl. J. Med.*, vol. 363, pp. 2301–2309,
1064 2010.
- 1065 [36] S. I. Chaudhry, Y. Wang, J. Concato *et al.*, "Patterns of weight
1066 change preceding hospitalization for heart failure," *Circulation*, vol. 116,
1067 pp. 1549–1554, 2007.
- 1068 [37] J. Gomez-Clapers, A. Serra-Rocamora, R. Casanella *et al.*, "Uncertainty
1069 factors in time-interval measurements in ballistocardiography," in *Proc.
1070 19th IMEKO TC-4 Symp. 17th IWADC Workshop Adv. Instrum. Sens.
1071 Interoperability*, Barcelona, Spain, 2013, pp. 395–399.
- 1072 [38] R. Gonzalez-Landaeta, O. Casas, and R. Pallas-Areny, "Heart rate
1073 detection from an electronic weighing scale," *Phys. Meas.*, vol. 29,
1074 pp. 979–988, 2008.
- [39] J. H. Shin, K. M. Lee, and K. S. Park, "Non-constrained monitoring
1075 of systolic blood pressure on a weighing scale," *Phys. Meas.*, vol. 30,
1076 pp. 679–693, 2009.
- [40] J. Alihanka, K. Vaahtoranta, and I. Saarikivi, "A new method for long-
1078 term monitoring of the ballistocardiogram, heart rate, and respiration,"
1079 *Amer. J. Physiol.*, vol. 240, pp. R384–R392, 1981.
- [41] Y. Chee, J. Han, and K. S. Park, "Air mattress sensor system with bal-
1081 ancing tube for unconstrained measurement of respiration and heart beat
1082 movements," *Phys. Meas.*, vol. 26, pp. 413–422, 2005.
- [42] D. C. Mack, J. T. Patrie, P. M. Suratt *et al.*, "Development and preliminary
1084 validation of heart rate and breathing rate detection using a passive,
1085 ballistocardiography-based sleep monitoring system," *IEEE Trans Inf.
1086 Technol. Biomed.*, vol. 13, no. 1, pp. 111–120, Jan. 2009.
- [43] A. Vehkaoja, S. Rajala, P. Kumpulainen *et al.*, "Correlation approach for
1088 the detection of the heartbeat intervals using force sensors placed under
1089 the bed posts," *J. Med. Eng. Technol.*, vol. 37, pp. 327–333, 2013.
- [44] B. H. Choi, G. S. Chung, J.-S. Lee *et al.*, "Slow-wave sleep estimation
1091 on a load cell installed bed: A non-constrained method," *Phys. Meas.*,
1092 vol. 30, pp. 1163–1170, 2009.
- [45] Y. Zhu, H. Zhang, M. Jayachandran *et al.*, "Ballistocardiography with
1094 fiber optic sensor in headrest position: A feasibility study and a new
1095 processing algorithm," in *Proc. 35th IEEE Annu. Int. Conf. Eng. Med.
1096 Biol. Soc.*, 2013, pp. 5203–5206.
- [46] S. Sprager and D. Zazula, "Heartbeat and respiration detection from
1098 optical interferometric signals by using a multimethod approach," *IEEE
1099 Trans. Biomed. Eng.*, vol. 59, no. 10, pp. 2922–9, Oct. 2012.
- [47] L. Dziuda and F. Skibniewski, "Monitoring respiration and cardiac activ-
1101 ity using fiber Bragg grating-based sensor," *IEEE Trans. Biomed. Eng.*,
1102 vol. 59, no. 7, pp. 1934–42, Jul. 2012.
- [48] J. M. Kortelainen and J. Virkkala, "FFT averaging of multichannel BCG
1104 signals from bed mattress sensor to improve estimation of heart beat
1105 interval," in *Proc. IEEE 29th Annu. Int. Conf. Eng. Med. Biol. Soc.*,
1106 2007, pp. 6685–6688.
- [49] J. Paalasmaa, M. Waris, H. Toivonen *et al.*, "Unobtrusive online moni-
1108 toring of sleep at home," in *Proc. IEEE Annu. Int. Conf. Eng. Med. Biol.
1109 Soc.*, 2012, pp. 3784–3788.
- [50] F. Wang, M. Tanaka, and S. Chonan, "Development of a PVDF piezopoly-
1111 mer sensor for unconstrained in-sleep cardiorespiratory monitoring,"
1112 *J. Intell. Mater. Syst. Struct.*, vol. 14, pp. 185–190, 2003.
- [51] C. Bruser, K. Stadlthanner, S. De Waele *et al.*, "Adaptive beat-to-beat
1114 heart rate estimation in ballistocardiograms," *IEEE Trans Inf. Technol.
1115 Biomed.*, vol. 15, no. 5, pp. 778–786, Sep. 2011.
- [52] K. Watanabe, T. Watanabe, H. Watanabe *et al.*, "Noninvasive measure-
1117 ment of heartbeat, respiration, snoring and body movements of a subject
1118 in bed via a pneumatic method," *IEEE Trans. Biomed. Eng.*, vol. 52,
1119 no. 12, pp. 2100–07, Dec. 2005.
- [53] X. Zhu, W. Chen, T. Nemoto *et al.*, "Real-time monitoring of respiration
1121 rhythm and pulse rate during sleep," *IEEE Trans. Biomed. Eng.*, vol. 53,
1122 no. 12, pp. 2553–63, Dec. 2006.
- [54] J. Kortelainen, M. V. Gils, and J. Parkka, "Multichannel bed pressure
1124 sensor for sleep monitoring," presented at the *Comput. Cardiol. Conf.*,
1125 Kraków, Poland, 2012.
- [55] C. Brueser, A. Kerekes, S. Winter *et al.*, "Multi-channel optical sensor-
1127 array for measuring ballistocardiograms and respiratory activity in bed,"
1128 presented at the *IEEE 34th Ann. Int. Conf. Eng. Med. Biol. Soc.*, San
1129 Diego, CA, USA, 2012.
- [56] T. Watanabe and K. Watanabe, "Noncontact method for sleep stage esti-
1131 mation," *IEEE Trans. Biomed. Eng.*, vol. 51, no. 10, pp. 1735–1748, Oct.
1132 2004.
- [57] D. W. Jung, S. H. Hwang, H. N. Yoon *et al.*, "Nocturnal awakening
1134 and sleep efficiency estimation using unobtrusively measured ballisto-
1135 cardiogram," *IEEE Trans. Biomed. Eng.*, vol. 61, no. 1, pp. 131–138, Jan.
1136 2014.
- [58] J. M. Kortelainen, M. O. Mendez, A. M. Bianchi *et al.*, "Sleep staging
1138 based on signals acquired through bed sensor," *IEEE Trans Inf. Technol.
1139 Biomed.*, vol. 14, no. 3, pp. 776–785, May 2010.
- [59] M. Migliorini, A. M. Bianchi, Nistico *et al.*, "Automatic sleep staging
1141 based on ballistocardiographic signals recorded through bed sensors," in
1142 *Proc. IEEE Annu. Int. Conf. Eng. Med. Biol. Soc.*, 2010, pp. 3273–3276.
- [60] K. Tanida, M. Shibata, and M. M. Heitkemper, "Sleep stage assessment
1144 using power spectral indices of heart rate variability with a simple algo-
1145 rithm: limitations clarified from preliminary study," *Biol. Res. Nursing*,
1146 vol. 15, pp. 264–272, 2013.
- [61] T. Koivistoinen, S. Junnila, A. Varri *et al.*, "A new method for measuring
1148 the ballistocardiogram using EMFi sensors in a normal chair," in *Proc.
1149 IEEE 26th Annu. Int. Conf. Eng. Med. Biol. Soc.*, 2004, pp. 2026–2029.

- [62] M. Walter, B. Eilebrecht, T. Wartzek *et al.*, "The smart car seat: Personalized monitoring of vital signs in automotive applications," *Pers. Ubiquitous Comput.*, vol. 15, pp. 707–715, 2011.
- [63] Y. Lim, K. Hong, K. Kim *et al.*, "Monitoring physiological signals using noninvasive sensors installed in daily life equipment," *Biomed. Eng. Lett.*, vol. 1, pp. 11–20, 2011.
- [64] B. H. Jansen, B. H. Larson, and K. Shankar, "Monitoring of the ballistocardiogram with the static charge sensitive bed," *IEEE Trans. Biomed. Eng.*, vol. 38, no. 8, pp. 748–751, Aug. 1991.
- [65] J. H. Shin, B. H. Choi, Y. G. Lim *et al.*, "Automatic ballistocardiogram (BCG) beat detection using a template matching approach," in *Proc. IEEE 30th Annu. Int. Conf. Eng. Med. Biol. Soc.*, 2008, pp. 1144–1146.
- [66] D. Friedrich, X. L. Aubert, H. Fuhr *et al.*, "Heart rate estimation on a beat-to-beat basis via ballistocardiography—a hybrid approach," presented at the *IEEE 32nd Annu. Int. Conf. Eng. Med. Biol. Soc.*, Buenos Aires, Argentina, 2010.
- [67] S. Sprager and D. Zazula, "Optimization of heartbeat detection in fiberoptic unobtrusive measurements by using maximum a posteriori probability estimation," *IEEE J. Biomed. Health Informat.*, vol. 18, no. 4, pp. 1161–1168, Jul. 2014.
- [68] W. Xu, W. A. Sandham, A. C. Fisher *et al.*, "Detection of the seismocardiogram W complex based on multiscale edges," presented at the *18th Annu. Int. Conf. IEEE EMBS (EMBC)*, Amsterdam, The Netherlands, 1996.
- [69] C. Bruser, J. M. Kortelainen, S. Winter *et al.*, "Improvement of force-sensor-based heart rate estimation using multi-channel data fusion," *IEEE J. Biomed. Health Informat.*, 2014, to be published.
- [70] J. Paalasmaa, H. Toivonen, and M. Partinen, "Adaptive heartbeat modelling for beat-to-beat heart rate measurement in ballistocardiograms," *IEEE J. Biomed. Health Informat.*, 2014, to be published.
- [71] C. Brueser, S. Winter, and S. Leonhardt, "Robust inter-beat interval estimation in cardiac vibration signals," *Phys. Meas.*, vol. 34, pp. 123–138, 2013.
- [72] J. H. Shin, S. H. Hwang, M. H. Chang, *et al.*, "Heart rate variability analysis using a ballistocardiogram during Valsalva manoeuvre and post exercise," *Phys. Meas.*, vol. 32, pp. 1239–1264, 2011.
- [73] X. Zhu, W. Chen, K. Kitamura *et al.*, "Comparison of pulse rate variability indices estimated from pressure signal and photoplethysmogram," in *Proc. IEEE Int. Conf. Biomed. Health Informat.*, 2012, pp. 867–870.
- [74] C. Brueser, S. Winter, and S. Leonhardt, "Unsupervised heart rate variability estimation from ballistocardiograms," presented at the *7th Int. Workshop Biosignal Interpretation*, Como, Italy, 2012.
- [75] O. T. Inan and G. T. A. Kovacs, "A low noise ac-bridge amplifier for ballistocardiogram measurement on an electronic weighing scale," *Phys. Meas.*, vol. 31, pp. N51–N59, 2010.
- [76] R. Wiard, O. Inan, B. Argyres *et al.*, "Automatic detection of motion artifacts in the ballistocardiogram measured on a modified bathroom scale," *Med. Biol. Eng. Comput.*, vol. 49, pp. 213–220, 2011.
- [77] K. Pandia, S. Ravindran, R. Cole *et al.*, "Motion artifact cancellation to obtain heart sounds from a single chest-worn accelerometer," presented at the *IEEE Int. Conf. Acoust., Speech, Signal Process.*, Dallas, TX, USA, 2010.
- [78] O. T. Inan, M. Etemadi, B. Widrow *et al.*, "Adaptive cancellation of floor vibrations in standing ballistocardiogram measurements using a seismic sensor as a noise reference," *IEEE Trans. Biomed. Eng.*, vol. 57, no. 3, pp. 722–727, Mar. 2010.
- [79] I. Starr and S. Ogawa, "On the aging of the heart; why is it so much more conspicuous in the ballistocardiogram than in the pulse?" *Amer. J. Med. Sci.*, vol. 242, pp. 399–410, 1961.
- [80] O. T. Inan, G. T. A. Kovacs, and L. Giovannardi, "Evaluating the lower-body electromyogram signal acquired from the feet as a noise reference for standing ballistocardiogram measurements," *IEEE Trans. Inf. Technol. Biomed.*, vol. 14, no. 5, pp. 1188–1196, Sep. 2010.
- [81] R. M. Wiard, O. T. Inan, L. Giovannardi *et al.*, "Preliminary results from standing ballistocardiography measurements in microgravity," in *Proc. IEEE 35th Annu. Int. Conf. Eng. Med. Biol. Soc.*, 2013, pp. 7290–7293.
- [82] I. Starr and A. Noordergraaf, *Ballistocardiography in Cardiovascular Research: Physical Aspects of the Circulation in Health and Disease*. Philadelphia, PA, USA: Lippincott, 1967.
- [83] V. Gurev, K. Tavakolian, J. Constantino *et al.*, "Mechanisms underlying isovolumic contraction and ejection peaks in seismocardiogram morphology," *J. Med. Biol. Eng.*, vol. 32, pp. 103–110, 2012.
- [84] Y. Henderson, "The mass movements of the circulation as shown by a recoil curve," *Amer. J. Phys.*, vol. 14, pp. 287–298, 1905.
- [85] W. R. Scarborough, S. A. Talbot, J. R. Braunstein *et al.*, "Proposals for ballistocardiographic nomenclature and conventions: revised and extended: Report of committee on ballistocardiographic terminology," *Circulation*, vol. 14, pp. 435–450, 1956.
- [86] N. Westerhof, F. Bosman, C. J. De Vries *et al.*, "Analog studies of the human systemic arterial tree," *J. Biomech.*, vol. 2, pp. 121–134, 1969.
- [87] J. Palladino, J. P. Mulier, F. Wu, *et al.*, "Assessing in the state of the circulatory system via parameters versus variables," *Cardiovasc. Diagn. Proc.*, vol. 13, pp. 131–139, 1996.
- [88] O. T. Inan, M. Etemadi, A. Paloma *et al.*, "Non-invasive cardiac output trending during exercise recovery on a bathroom-scale-based ballistocardiogram," *Physiol. Meas.*, vol. 30, pp. 261–274, 2009.
- [89] M. Etemadi, O. T. Inan, L. Giovannardi *et al.*, "Rapid assessment of cardiac contractility on a home bathroom scale," *IEEE Trans. Inf. Technol. Biomed.*, vol. 15, no. 6, pp. 864–869, Nov. 2011.
- [90] E. Pinheiro, O. Postolache, and P. Girao, "Pulse arrival time and ballistocardiogram application to blood pressure variability estimation," in *Proc. IEEE Int. Workshop Med. Meas. Appl.*, 2009, pp. 132–136.
- [91] R. Casanella, J. Gomez-Clapers, and R. Pallas-Areny, "On time interval measurements using BCG," in *Proc. IEEE Annu. Int. Conf. Eng. Med. Biol. Soc.*, 2012, pp. 5034–5037.
- [92] K. Tavakolian, G. Houlton, G. A. Durmont *et al.*, "Precordial vibrations provide noninvasive detection of early-stage hemorrhage," *J. Shock*, vol. 41, pp. 91–96, 2014.
- [93] M. Di Rienzo, E. Vaini, P. Castiglioni *et al.*, "Beat-to-beat estimation of LVET and QS2 indices of cardiac mechanics from wearable seismocardiography in ambulant subjects," in *Proc. IEEE 35th Annu. Int. Conf. Eng. Med. Biol. Soc.*, 2013, pp. 7017–7020.
- [94] S. M. Munir, R. C. Boganev, E. Sobash *et al.*, "Devices in heart failure: Potential methods for device-based monitoring of congestive heart failure," *Texas Heart Inst. J.*, vol. 35, pp. 166–173, 2008.
- [95] *ClinicalTrials.gov*. [Online]. Available: <http://clinicaltrials.gov/show/NCT01121107>
- [96] J. Zanetti and D. Salerno, "Seismocardiography: A new technique for recording cardiac vibrations. concept, method, and initial observations," *J. Cardiovasc. Technol.*, vol. 9, pp. 111–120, 1990.
- [97] A. M. Weissler, W. S. Harris, and C. D. Schoenfeld, "Systolic time intervals in heart failure in man," *Circulation*, vol. 37, pp. 149–159, 1968.
- [98] C. L. Garrard, A. M. Weissler, and H. T. Dodge, "The relationship of alterations in systolic time intervals to ejection fraction in patients with cardiac disease," *Circulation*, vol. 42, pp. 455–462, 1970.
- [99] D. M. Salerno, J. M. Zanetti, L. A. Green *et al.*, "Seismocardiographic changes associated with obstruction of coronary blood flow during balloon angioplasty," *Amer. J. Cardiol.*, vol. 68, pp. 201–207, 1991.
- [100] D. Salerno, J. M. Zanetti, L. Poliac *et al.*, "Exercise seismocardiography for detection of coronary artery disease," *Amer. J. Noninvasive Cardiol.*, vol. 6, pp. 321–330, 1992.
- [101] M. Jerosch-Herold, J. Zanetti, H. Merkle *et al.*, "The seismocardiogram as magnetic-field-compatible alternative to the electrocardiogram for cardiac stress monitoring," *Int. J. Cardiac Imag.*, vol. 15, pp. 523–531, 1999.
- [102] F. I. Marcus, V. Sorrell, J. Zanetti *et al.*, "Accelerometer-derived time intervals during various pacing nodes in patients with biventricular pacemakers: Comparison with normals," *Pacing Clin. Electrophysiol.*, vol. 30, pp. 1476–1481, 2007.
- [103] B. Silke, J. Spiers, N. Herity *et al.*, "Seismocardiography during pharmacodynamic intervention in man," *Automedica*, vol. 16, pp. 35–44, 1994.
- [104] J. R. Libonati, J. Ciccolo, and J. Glassberg, "The tei index and exercise capacity," *J. Sports Med.*, vol. 41, pp. 108–113, 2001.
- [105] J. M. Zanetti and K. Tavakolian, "Seismocardiography: Past, present, and future," presented at the *IEEE Eng. Med. Biol. Soc. Conf.*, Osaka, Japan, 2013.
- [106] E. Pinheiro, O. Postolache, and P. Girao, "Theory and developments in an unobtrusive cardiovascular system representation: Ballistocardiography," *Open Biomed. Eng. J.*, vol. 4, pp. 201–216, 2010.
- [107] O. Postolache, P. S. Girao, J. Mendes *et al.*, "Unobtrusive heart rate and respiratory rate monitor embedded on a wheelchair," in *Proc. IEEE Int. Workshop Med. Meas. Appl.*, 2009, pp. 83–88.
- [108] A. Akhbardeh, K. Tavakolian, V. Gurev *et al.*, "Comparative analysis of three different modalities for characterization of the seismocardiogram," in *Proc. IEEE Annu. Int. Conf. Eng. Med. Biol. Soc.*, 2009, pp. 2899–2903.

- 1301 [109] C. Bruser, J. Diesel, M. D. H. Zink *et al.*, "Automatic detection of
1302 atrial fibrillation in cardiac vibration signals," *IEEE J. Biomed. Health*
1303 *Informat.*, vol. 17, pp. 162–171, 2013.
- 1304 [110] L. Giovangrandi, O. T. Inan, D. Banerjee *et al.*, "Preliminary results from
1305 BCG and ECG measurements in the heart failure clinic," in *Proc. IEEE*
1306 *Eng. Med. Biol. Soc. Annu. Int. Conf.*, 2012, pp. 3780–3783.
- 1307 [111] A. I. Hernandez, F. Ziglio, A. Amblard *et al.*, "Analysis of endocardial
1308 acceleration during intraoperative optimization of cardiac resynchroniza-
1309 tion therapy," in *Proc. IEEE 35th Annu. Int. Conf. Eng. Med. Biol. Soc.*,
1310 2013, pp. 7000–7003.
- 1311 [112] A. Scano and M. Strollo, "Ballistocardiographic research in weightless-
1312 ness," *Earth-Orient Appl. Space Technol.*, vol. 15, pp. 101–104, 1985.
- 1313
- [113] G. K. Prisk and P. F. Migeotte, "Physiological insights from gravity-free
ballistocardiography," in *Proc. IEEE 35th Annu. Int. Conf. Eng. Med.*
Biol. Soc., 2013, pp. 7282–7285.
- [114] R. M. Baevsky, I. I. Funtova, E. S. Luchitskaya *et al.*, "Microgravity: An
ideal environment for cardiac force measurements," *Cardiometry Open*
Access e-J., vol. 3, pp. 100–117, 2013.
- Authors' photographs and biographies not available at the time of publication.

IEEE
PROOF

QUERIES

1322

- Q1. Author the abbreviation “EMFi” has been used for two terms, i.e., electromagnetic film and electromechanical film in the text. Please check. 1323
1324
- Q2. Author: Please provide names of all authors in place of et al. in Refs. [1], [7], [8], [11]–[15], [17]–[19], [21], [22], [24]–[29], [32], [35]–[37], [42]–[45], [49], [51]–[53], [55], [57]–[59], [61]–[63], [65], [66], [68], [69], [72], [73], [76]–[78], [81], [83], [85]–[89], [92]–[94], [99]–[103], [107]–[111], and [114]. 1325
1326
1327
- Q3. Author: Please provide the technical report number in Ref. [9]. 1328
- Q4. Author: Please provide the page range in Ref. [23]. 1329
- Q5. Author: Please update Refs. [69] and [70], if possible. 1330
- Q6. Author: Please provide the year in Ref. [95]. 1331

IEEE
Proof

Ballistocardiography and Seismocardiography: A Review of Recent Advances

Omer T. Inan, *Member, IEEE*, Pierre-Francois Migeotte, *Member, IEEE*, Kwang-Suk Park, *Senior Member, IEEE*,
Mozziyar Etemadi, *Student Member, IEEE*, Kouhyar Tavakolian, *Member, IEEE*, Ramon Casanella, *Member, IEEE*,
John Zanetti, Jens Tank, Irina Funtova, G. Kim Prisk, *Senior Member, IEEE*, and Marco Di Rienzo, *Member, IEEE*

Abstract—In the past decade, there has been a resurgence in the field of unobtrusive cardiomechanical assessment, through advancing methods for measuring and interpreting ballistocardiogram (BCG) and seismocardiogram (SCG) signals. Novel instrumentation solutions have enabled BCG and SCG measurement outside of clinical settings, in the home, in the field, and even in microgravity. Customized signal processing algorithms have led to reduced measurement noise, clinically relevant feature extraction, and signal modeling. Finally, human subjects physiology studies have been conducted using these novel instruments and signal processing tools with promising clinically relevant results. This paper reviews the recent advances in these areas of modern BCG and SCG research.

Index Terms—Ballistocardiogram (BCG), cardiomechanical signals, noninvasive physiologic monitoring, seismocardiogram (SCG), ubiquitous health.

Manuscript received May 14, 2014; revised August 20, 2014; accepted September 29, 2014. Date of publication; date of current version. The work of P. F. Migeotte was supported by the Belgian Federal Science Policy Office via the European Space Agency PRODEX program (ILSRA-2009-0729). The work of G. K. Prisk was supported by the National Space Biomedical Research Institute through NASA NCC9-58. The work of J. Tank and I. I. Funtova were supported by the German Space Agency (DLR) under Grant 50WB1117. The work of M. Di Rienzo was supported in part by the Italian Space Agency through ASI 2013-061-I.0 and ASI 2013-079-R.0.

O. T. Inan is with the School of Electrical and Computer Engineering, Georgia Institute of Technology, Atlanta, GA 30308 USA (e-mail: oeinan@gmail.com).

P.-F. Migeotte is with the Department of Cardiology, Universite Libre de Bruxelles 1050, Brussels, Belgium (e-mail: Pierre-Francois.Migeotte@ulb.ac.be).

K.-S. Park is with the Department of Biomedical Engineering, Seoul National University, Seoul 110-799, Korea (e-mail: kspark@bmsil.snu.ac.kr).

M. Etemadi is with the Department of Bioengineering and Therapeutic Sciences, University of California at San Francisco, San Francisco, CA 94143 USA (e-mail: mozziyar.emetadi@ucsf.edu).

K. Tavakolian is with the Department of Electrical Engineering, University of North Dakota, Grand Forks, ND 58202 USA (e-mail: kouhyart@gmail.com).

R. Casanella is with the Instrumentation, Sensors, and Interfaces Group, Universitat Politècnica de Catalunya, 08034 Barcelona, Spain (e-mail: ramon.casanella@upc.edu).

J. Zanetti is with Acceleron Medical Systems, Arkansaw, WI 54721 USA (e-mail: jmzsenior@gmail.com).

J. Tank is with the Klinische Pharmakologie, Medizinische Hochschule Hannover, 30625 Hannover, Germany (e-mail: Tank.Jens@mh-hannover.de).

I. Funtova is with the Laboratory for Autonomic Regulation of Cardiorespiratory System, Institute of Biomedical Problems, Russian Academy of Sciences, 123007 Moscow, Russian (e-mail: funtova.imbp@mail.ru).

G. K. Prisk is with the Department of Medicine and Radiology, University of California at San Diego, La Jolla, CA, 92093 USA (e-mail: kprisk@ucsd.edu).

M. Di Rienzo is with the Department of Biomedical Technology, Fondazione Don Carlo Gnocchi, ONLUS, 20133 Milano, Italy (e-mail: mdrienzio@dongnocchi.it).

Color versions of one or more of the figures in this paper are available online at <http://ieeexplore.ieee.org>.

Digital Object Identifier 10.1109/JBHI.2014.2361732

I. INTRODUCTION

As detailed in the following sections, the ballistocardiogram (BCG) is a measurement of the recoil forces of the body in reaction to cardiac ejection of blood into the vasculature [1], while the seismocardiogram (SCG) represents the local vibrations of the chest wall in response to the heartbeat [2]. The BCG phenomenon was first observed in 1877 by Gordon, with the finding that, as a subject would stand on a weighing scale, the needle would vibrate synchronously to the subject's heartbeat [3]. Nearly 60 years later, Starr and colleagues created an instrument in the form of a table with a mobile top surface to measure the BCG in a repeatable scientific manner [1]. The SCG was first observed by Bozhenko in 1961, and was first applied in clinical studies 30 years later in 1991 by Salerno and Zanetti [4]. Throughout the 1900s, both BCG and SCG signals were heavily investigated and several publications appeared in major scientific and clinical journals (e.g., [4]–[7]). However, because of the advent of echocardiography and magnetic resonance imaging, and overly-cumbersome hardware, BCG and SCG were largely abandoned by the medical community [8].

Today, technological advancements largely simplify the measurement and assessment of these signals and open new perspectives in their clinical use. This paper reviews the instrumentation and signal processing advances which have helped to propel BCG and SCG into this revival. It also summarizes some of the key human subjects studies performed recently that support the use of BCG and SCG in extra-clinical applications.

II. DESCRIPTION OF BCG AND SCG SIGNALS

A. BCG Signal Description

At every heartbeat, the blood travelling along the vascular tree produces changes in the body center of mass. Body micromovements are then produced by the recoil forces to maintain the overall momentum. The BCG is the recording of these movements, can be measured as a displacement, velocity, or acceleration signal, and is known to include movements in all three axes. The longitudinal BCG is a measure of the head-to-foot deflections of the body, while the transverse BCG represents antero-posterior (or dorso-ventral) vibrations. The original bed- and table-based BCG systems focused on longitudinal BCG measurements, representing what was supposed to be the largest projection of the 3-D forces resulting from cardiac ejection [1]. Table I summarizes modern BCG measurement systems and their axes of measurement. Note that for some systems, head-to-foot and dorso-ventral forces are unavoidably, mixed

TABLE I
MODERN BCG SYSTEMS AND THEIR CORRESPONDING MEASUREMENT AXES

Modern BCG System	Axis	Comments / Challenges
Accel. (0g)	All (3-D)	- Needs reduced gravity
Accel. (1g)	Head-to-foot	- Placement affects signal shape and amplitude - Motion artifacts must be detected and mitigated
Bed	Head-to-foot or Dorso-ventral	- Cross-axis coupling - Changes in sleep position affect signal quality / shape
Chair	Head-to-foot or Dorso-ventral	- Posture affects signal quality and repeatability
Weighing Scale	Head-to-foot	- Posture affects signal quality and repeatability - Motion artifacts must be detected and mitigated

66 together in the measurement, and this should be accounted for
67 when interpreting results. However, in spite of the 3-D nature of
68 the BCG, for a long period of time only the microdisplacements
69 of the body along the longitudinal axis (head-to-foot) were con-
70 sidered. Currently, BCG is mainly measured using a force plate
71 or force sensor placed on a weighing scale or under the seat of a
72 chair, with the subject in a vertical position. Modern approaches
73 to BCG measurement are discussed below in Section III.

74 It should be considered, however, that the gravity force and
75 any contact of the body with external objects, including the
76 floor and measuring devices, somewhat interferes with, or even
77 impedes, the body displacement induced by the recoil forces.
78 As a result, the BCG measurement on earth is always affected
79 by some distortion. The ideal environment for assessing the
80 BCG would be in microgravity settings, such as during space
81 missions. Such experiments have been performed, and the re-
82 sults described below confirm that in microgravity the whole
83 body recoil forces (BCG) are significant in all three dimensions
84 [9]–[12]. Modeling studies examining the cardiogenic traction
85 forces of the aorta have confirmed this finding as well [13].

86 B. SCG Signal Description

87 SCG is the measure of the thoracic vibrations produced by the
88 heart's contraction and the ejection of blood from the ventricles
89 into the vascular tree. Today, the SCG can readily be detected
90 by placing a low-noise accelerometer on the chest. If a tri-axial
91 accelerometer is used, SCG components are present in all three
92 axes, each displaying a specific pattern [12], [14]. However, in
93 the literature, the majority of studies on SCG only focus on the
94 amplitude of the dorso-ventral component, although it is likely
95 that additional biological information could be derived also from
96 the analysis of the longitudinal and lateral SCG components, and
97 from the analysis of the acceleration vector trajectory during
98 the heart cycle. Unless the contrary is stated to be consistent
99 with the prevalent literature only the dorso-ventral acceleration
100 component of SCG will be considered in the remainder of this
101 paper.

102 C. BCG and SCG Waveforms

103 For each heart contraction, a BCG and SCG waveform is gen-
104 erated. Each waveform is characterized by several peaks and val-

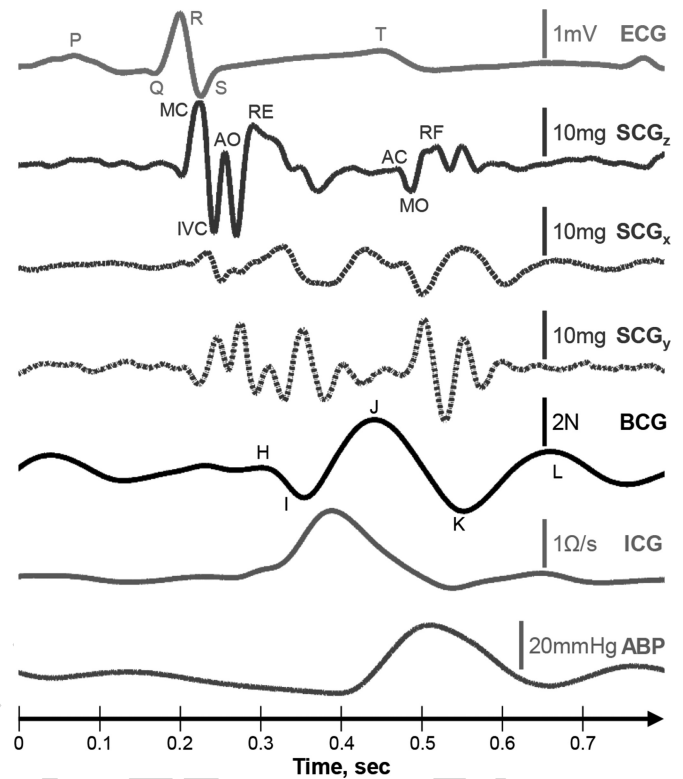


Fig. 1. Simultaneously acquired Lead II electrocardiogram (ECG); three-axis seismocardiogram (SCG) with z indicating the dorso-ventral axis, x indicating the right-to-left lateral axis, and y indicating the head-to-foot axis; ballistocardiogram (BCG); impedance cardiogram (ICG); and arterial blood pressure (ABP) measured at the finger, signals from one subject, illustrating the relative timing and amplitude features of the signals.

105 leys reflecting specific events of the beating heart. Fig. 1 shows a
106 typical ECG, head-to-foot BCG, tri-axial SCG, impedance car-
107 diogram (ICG), and arterial blood pressure (ABP) measurement
108 from a healthy subject (data were collected with approval from
109 the Institutional Review Board, IRB, at the Georgia Institute of
110 Technology, and with written informed consent obtained). A
111 high-resolution, miniature accelerometer was used for the SCG
112 data collection (356A32, PCB Piezotronics, Depew, NY, USA),
113 and a modified weighing scale was used for the BCG recording
114 as described previously in [15]. The ECG and ICG waveforms
115 were measured using the BN-RSPEC and BN-NICO wireless
116 units (BIOPAC Systems, Inc., Goleta, CA, USA) interfaced to
117 the MP150WSW data acquisition hardware (BIOPAC Systems,
118 Inc., Goleta, CA, USA). The ABP was measured from the fin-
119 ger using the A2SYS Nexfin Monitor (Edwards Lifesciences,
120 Irvine, CA, USA). For this measurement, z corresponded to the
121 dorso-ventral, y to the head-to-foot, and x to the right-to-left
122 lateral components of the SCG. The labels of the peaks and val-
123 leys of the dorso-ventral components shown in this figure are
124 according to [16], [17]; for the BCG, the labels are according
125 to [1]. For the SCG, the labels correspond to the physiological
126 event they are believed to represent: MC, mitral valve closure;
127 IVC, isovolumetric contraction; AO, aortic valve opening; RE,
128 rapid ejection; AC, aortic valve closure; MO, mitral valve open-
129 ing; and RF, rapid filling. For the BCG, the labels of the waves
130 are not associated directly with underlying events, but rather
131 the current understanding is that the waveform represents the

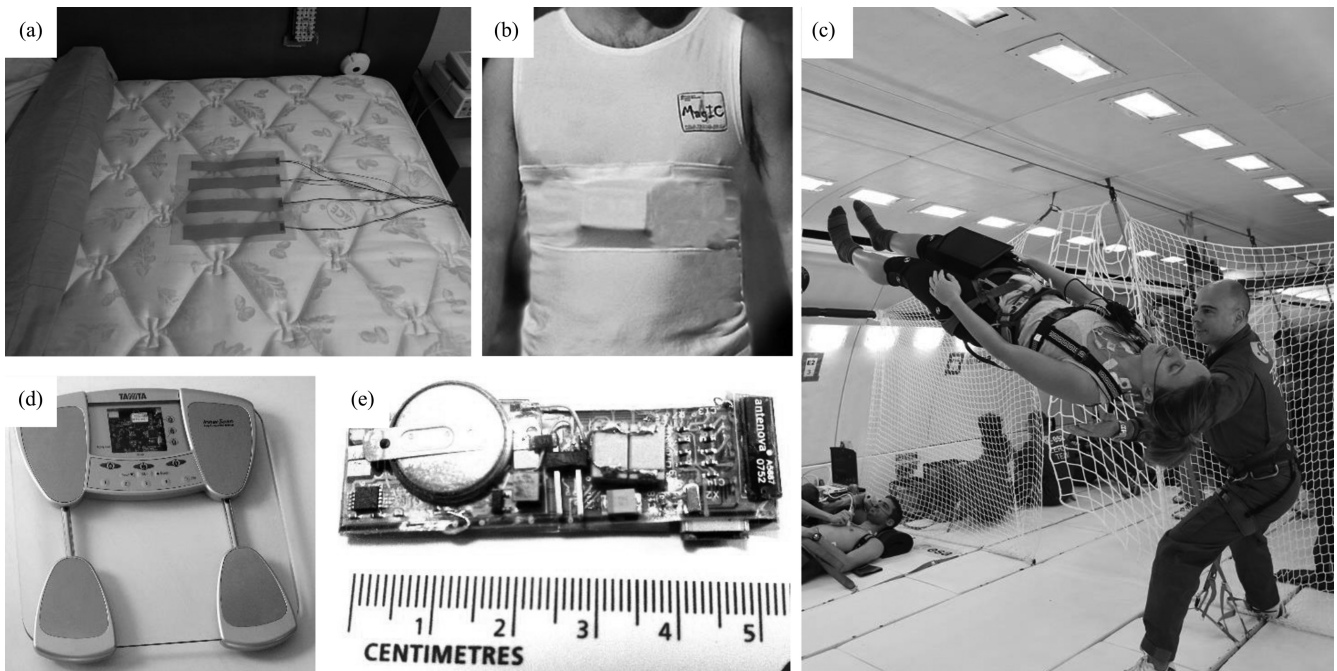


Fig. 2. Compilation of modern BCG and SCG acquisition hardware. (a) PVDF sensor installed into the bed for BCG measurements during sleep. (b) Tri-axial SCG measurement system built into the MagIC-SCG vest for continuous recordings during normal activities of daily living. Modified from [14] with permission. (c) Wearable 3-D BCG measurement hardware (Pneumocard) being used on board a parabolic flight for microgravity BCG measurements; Photo Credit: ESA. (d) Weighing scale with built in circuitry for BCG measurement from a standing subject. (e) Flexible hardware for chest-mounted tri-axial SCG measurements.

132 combined mechanical pulse response of the vasculature and
 133 body to cardiac ejection of blood [18]. Note that, when the
 134 BCG is measured by a scale or force plate, the SCG and BCG
 135 units are not the same; the SCG records the accelerations of
 136 the chest wall, and is thus presented in units of milligram; the
 137 BCG represents the displacements of the center of mass of
 138 the subject on the weighing scale, which are then converted
 139 to units of force by the spring constant for the scale platform,
 140 and thus it is presented in units of Newtons. The mass that is
 141 accelerated for the SCG is not the same as the mass acceler-
 142 ated for the BCG; as such, the direct conversion of the BCG to
 143 acceleration units or the SCG to force units has not yet been
 144 elucidated.

145 *D. Importance of Sensor Location, Axis Selection*
 146 *and Orientation*

147 For both BCG and SCG, the measurement location has a sig-
 148 nificant bearing on the morphology, amplitude, and clinically
 149 relevant features of the signal. For the SCG, since it is a mea-
 150 sure of local vibrations, the precise location of the sensor on
 151 the chest impacts the measured signal [19]–[21]. A widely used
 152 placement has been on the sternum [14], [22], [23]. Pandia *et al.*
 153 found that the second heart sound was more pronounced when
 154 the SCG was measured on the left side of the chest compared
 155 to the sternum [19]. For BCG signals measured using an ac-
 156 celerometer, the same is true; an accelerometer placed on the
 157 foot will not measure the same BCG signal as one placed on
 158 the head, thus stressing the importance of a clear description of,
 159 and thoughtfulness regarding, the sensor location on the body.

An additional crucial issue is the orientation of the acceleration
 axis. BCG or SCG accelerations in the dorso–ventral direction
 will not be identical to those in the lateral (right-to-left) or head-
 to-foot direction; consequently, depending on the purpose of
 the measurement the axis should be chosen accordingly or a
 three-axis accelerometer should be used.

In spite of the major role played by the selection of the mea-
 surement axes, the axes orientation, and the sensor location,
 from the review of the existing literature it appears that infor-
 mation on these aspects is often missing, making difficult the
 understanding of the experimental setup and the interpretation
 of results. Thus, as detailed in Section VI, a standardization
 on these issues is deemed necessary, and in the meantime, it
 is advisable that the above pieces of information are clearly
 stated in any scientific communication dealing with BCG and
 SCG.

III. INSTRUMENTATION: ENABLING UBIQUITOUS MONITORING

Fig. 2 shows a compilation of photos depicting several exam-
 ples of modern BCG and SCG acquisition hardware, enabling
 data acquisition in a variety of settings, including in bed, in
 the home, outdoors, and in microgravity. These systems are
 discussed below in detail.

A. *Wearable BCG or SCG Systems*

The primary advantage of wearable BCG or SCG mea-
 surement systems is the possibility of obtaining data contin-
 uously throughout normal daily living. Additionally, record-
 ings with wearable systems can potentially be acquired in any

187 environment; thus, providing an opportunity to assess a per-
 188 son's cardiovascular performance under various environmental
 189 settings or stressors.

190 The sensor type used most often for wearable BCG or SCG
 191 measurements is an accelerometer, typically with three-axis
 192 measurement capability, that is mechanically coupled to the
 193 body with either adhesives, plastic mounting, or textiles. In
 194 2007, Castiglioni *et al.* tested the SCG assessment by an ex-
 195 ternal three-axis MEMS accelerometer placed on the left clavi-
 196 cle, connected to a smart garment with textile ECG electrodes,
 197 thus obtaining simultaneous tri-axial SCG and single-lead ECG
 198 recordings [24]. The concept was subsequently refined, and in
 199 2010, Di Rienzo *et al.* proposed an integrated vest equipped with
 200 sensors, the MagIC-SCG device, in which the accelerometer
 201 was inside the system electronics and placed in contact with the
 202 subject's sternum [14]. Through this system, SCG was recorded
 203 over 24 h in ambulant subjects, while performing a variety of
 204 activities of normal daily living and beat-to-beat estimates of
 205 cardiac time intervals (CTIs) could be estimated [21]. Chuo
 206 *et al.* developed miniaturized hardware ($55 \times 15 \times 3$ mm) on
 207 a flexible substrate with adhesive backing for wireless tri-axial
 208 SCG recording from the sternum (also with a MEMS accelerom-
 209 eter) together with single-lead ECG and coarse single-point skin
 210 temperature via a thermistor [25]. Baevsky *et al.* developed a
 211 portable system, "Pneumocard," for the assessment of the car-
 212 diac function of cosmonauts on board the International Space
 213 Station [26]. The system comprised a single-axis MEMS ac-
 214 celerometer placed at the apex of the heart for the recording of
 215 the SCG signal. Later, a three-axis MEMS accelerometer was
 216 added to the system for the recording of the BCG signal. The
 217 accelerometer was placed on the back of the subject, either at
 218 the center of mass or between the scapulae and its performance
 219 during the microgravity phases of parabolic flights was tested
 220 by Migeotte *et al.* [27]–[29].

221 He *et al.* placed a tri-axial MEMS accelerometer for BCG
 222 measurement in a plastic mount over the ear, with auxiliary
 223 sensors include for ECG and / or photoplethysmogram (PPG)
 224 measurement, respectively, [30], [31]. Hyun *et al.* used an
 225 electromagnetic film (EMFi) patch to measure the vibrations
 226 of the chest wall in the dorso-ventral direction (transverse);
 227 however, it should be noted that the exact position on the
 228 chest for the measurement was not provided, and on the ba-
 229 sis of morphology, while the signal was called the BCG, it
 230 was likely rather an SCG [32]. Another notable approach—
 231 that is not exactly a wearable device, but provides some similar
 232 advantages—was demonstrated by Balakrishnan *et al.* with the
 233 head-to-foot (longitudinal) direction ballistocardiographic dis-
 234 placements of the head being captured and processed from video
 235 recordings [33].

236 B. Weighing Scale BCG

237 The first measurement of BCG on an electronic scale was
 238 demonstrated in 1990 by Jim Williams of Linear Technology, as
 239 described in his application note AN-43 [34]. Williams built an
 240 elegant circuit capable of measuring bodyweight with tremen-
 241 dous accuracy—4.5 g resolution up to 136 kg—and found mo-

tion artifacts, and the BCG as the largest sources of noise for
 his measurements.

242 The main advantage with weighing-scale-based BCG mea-
 243 surement is that the subject is standing up for the measurement—
 244 ironically, this is also the main disadvantage. While the standing
 245 posture of the subject is ideal for ensuring that the measurement
 246 is purely longitudinal, it also means the measurements are sus-
 247 ceptible to motion artifacts and floor vibrations. This also places
 248 a practical limit on the duration of the measurements, as the pa-
 249 tient will likely only stand still on the scale for 30–60 s at a time at
 250 most. Another key advantage of these systems is that they lever-
 251 age the tremendous popularity of weighing scales, with more
 252 than 80% of American households owning a scale, and multiple
 253 companies developing new and improved "smart" scales with
 254 enhanced capabilities. The scale is also used by heart failure pa-
 255 tients at home to monitor increasing trends in their bodyweight,
 256 which may be related to increased fluid retention [35], [36].

257 With these potential advantages in mind, researchers have
 258 rigorously investigated this mode of BCG measurement. Inan
 259 *et al.* measured the mechanical frequency response of several
 260 commercially available scales at various loads to determine if
 261 the bandwidth was sufficient for BCG recording over a wide
 262 range of bodyweight. For bodyweights up to 160 kg, they found
 263 that the mechanical systems of most commercial scales have
 264 a bandwidth exceeding 15 Hz, which is sufficient for BCG
 265 measurement [15]. Note that for preserving the accuracy of
 266 time interval detection from the BCG, such as the R–J interval
 267 between the ECG and BCG, analog and digital low-pass filtering
 268 operations should not use a cutoff frequency lower than 25 Hz
 269 [37]. BCG measurement on a scale has also been successfully
 270 demonstrated by Gonzalez-Landaeta *et al.* [38] and Shin *et al.*
 271 [39], and in all studies the shape and amplitude of the signal is
 272 very similar to the traditional BCG recordings taken by Starr
 273 *et al.* nearly a century earlier [1].

276 C. Bed-Based BCG Systems

277 BCG can be applied in evaluating the sleep stages and sleep
 278 related disorders in more comfortable environment replacing
 279 some functions done by polysomnography (PSG). Since BCG-
 280 based technology does not require attaching electrodes on pa-
 281 tient body surface, it has advantage over ECG of not disturb-
 282 ing subject's ordinary sleep behaviors in collecting data. BCG
 283 measurement can be integrated with the subject's sleeping en-
 284 vironment using several types of sensors, the first of which was
 285 a static charge sensitive bed by Alihanka *et al.* [40], and more
 286 recently the following implementations: Pressure sensor in the
 287 air mattress [41] or in pad [42], film-type force sensors [43] or
 288 load cells in the legs of bed [44], microbend fiber optic BCG
 289 sensor [45]–[47], EMFi sensors [48], piezoelectric film sensors
 290 [49] or polyvinylidene fluoride (PVDF) sensors [50] in the mat-
 291 tress pad, strain gauges [51], pneumatic [52], and hydraulic [53]
 292 sensors. Some researchers have also proposed the use of sensor
 293 arrays rather than single sensors to improve robustness [54],
 294 [55]. As these sensors can usually provide the additional infor-
 295 mation on respiration and body movement as well as heart beats,
 296 this information can be incorporated with the BCG to generate

sleep evaluating parameters more accurately, as well as other applications such as early warning in the general ward, or home monitoring, where rhythm and dynamics can be monitored over extended periods of time for predictive analytics.

Sleep stages have mainly been classified into two levels slow wave sleep or non-slow wave sleep (SWS/non-SWS), or three levels (wake/REM/NREM) based on BCG. The earliest implementation of BCG based sleep staging was by Watanabe and Watanabe [56]. Two stage classification between SWS and non-SWS was performed based on BCG with movement measured unobtrusively by a load cell installed bed [44]. Based on calculated heart rate variability (HRV) parameters, they achieved the mean agreement of 92.5% (kappa index of 0.62). Sleep efficiency was evaluated by detecting nocturnal awakening epochs in BCG measured using PVDF sensors on bed mattress [57], based on the principle that awakening during sleep is related with subtle changes in heart rate; thus, awakening epochs can be detected based on HRV parameters. They achieved the classification accuracy of 97.4% (kappa index of 0.83) and 96.5% (kappa index of 0.81) and evaluated the sleep efficiency with absolute error of 1.08% and 1.44% for normal subjects and obstructive sleep apnea patients, respectively.

Three stage classification (Wake/REM/NREM) of sleep has been derived using the analyses of spectral components of the heartbeats extracted from multichannel BCG based on EMFi sensors [58]. By applying a hidden Markov model only on BCG, they achieved a total accuracy of 79% (kappa index of 0.43) compared to clinical sleep staging from PSG. The performance was enhanced by combining the time variant-autoregressive model (TVAM) and wavelet discrete transform (WDT) with the quadratic (QD) or linear discriminant (LD) analysis [59]. The QD-TVAM algorithm achieved a total accuracy of 76.8% (kappa index of 0.55), while LD-WDT achieved a total accuracy of 79% (kappa index of 0.51). Although there was also a study done for sleep stage classification into four levels (wake/REM/deep sleep/light sleep) with ECG [60], four-level sleep stage classification with BCG is not reported yet. With the ECG signal, Tanida *et al.* classified the sleep stage with HRV analyzed for each 60-s epoch of ECG and calculated at three frequency band powers. Their results for minute-by minute agreement rate ranged from 32% to 72% with an average of 56% for ten healthy women.

Sleep monitoring based on BCG technology has a potential to provide both continuous and longitudinal information on a subjects' sleep quality and may take a role as a predictive screening method prior to the sleep studies based on PSG. It could also fill the gap among PSG of whole night examination and portable ambulatory PSG, which can be applied at home and simplified with, for example, a wrist worn movement sensor.

D. Chair-Based BCG and SCG systems

Chair-based systems have mainly used electromechanical film (EMFi) sensors based on piezoelectric transduction. Koivisto *et al.* attached EMFi sensors to a chair to measure BCG signals from two seated subjects, and found the signal shape to be similar to other BCG measurements from the literature

[61]. Walter *et al.* placed an EMFi mat in the cushion of the driver's seat in a car to measure the BCG for automatically monitoring driver fitness [62]. These systems provide a means for measuring BCG or SCG signals from patients who cannot stand still on their own, minimize motion artifacts, and allow the user to be comfortable during the measurement. The main disadvantages for chair-based BCG recording are the reduction of signal amplitude compared to measurements using table, bed, or weighing scale systems, and the effects of postural changes on signal quality.

IV. SIGNAL PROCESSING AND MODELING

A. Heartbeat Detection

Since heart rate is regulated by the autonomic nervous system, the analysis of HRV is currently employed to obtain physiological and clinical information on the level of sympathetic and parasympathetic drive to the heart. Even though ECG is the most widely used biological signal to evaluate heart rate dynamics, BCG may also be used. Due to its easier application for monitoring in contrast to the inconvenience of attaching electrodes to the skin in ECG measurement, BCG may facilitate the assessment of heart rate dynamics in daily life [63].

Heartbeats may be identified by the J-wave peak in the BCG signal, i.e., the point of highest amplitude in the BCG waveform. Heart rate is evaluated by measuring the interval between consecutive J-peaks, the J-J interval. As there are many algorithms to detect the R-peak in ECG, there are also various methods to detect the J-peaks or heart beat from BCG. Since BCG can be measured in different settings with different type of sensors, the peak-detection algorithm should be selected to optimize the performance considering the characteristics of measured BCG. A heartbeat detection algorithm which showed high performance in R-peak detection from ECG can be applied with minor modification for J-peak detection. Generally the peak detection procedure is applied to select the highest value in amplitude as the J-peak within the sliding window after some preprocessing to increase signal-to-noise ratio (SNR) and to reject artifacts due to motion or other interferences.

Choi *et al.* demonstrated increased detection performance with a dedicated algorithm, which finds local peaks in four divided subintervals within a period and selects the maximum peak as J-peak from these local peaks with some rejection rules [44]. Jansen *et al.* applied a detection method based on a "template matching" rule by evaluating a correlation function in a local moving window [64], a method which was further refined and developed by Shin *et al.* [65]. Although this method requires template design in its first stage, Shin *et al.* successfully applied it to several types of BCG signals acquired from air mattress, load cells, and EMFi sensors. The results showed 95.2% of sensitivity and 94.8% of specificity in average for five subjects and three types of BCG signals. Additional methods for heartbeat detection from BCG signals include those which combine different estimators [46], [66], [67], and methods which use wavelets to preprocess the signal prior to peak detection [53], [68].

Heart rate was estimated from the spectral domain specially focusing on third harmonics especially in BCG signals acquired

with fiber optic sensors [45]. The results showed an error less than 0.34 beat/min in 2°min averaged heart rate. Heartbeat intervals were calculated with the cepstrum method, by applying FFT for short time windows including pair of consequent heart beats [48]. Relative error of the method was 0.35% for 15 night recordings with six normal subjects after rejecting movement artifacts. Since the results of heart beat detection are not perfect, generally visual editing is required to correct the errors in peak detection for further application like HRV analysis. Multi-channel fusion techniques have also been demonstrated recently for BCG-based heartbeat detection [48], [69].

Recently, Paalasmaa *et al.* [70] and Brueser *et al.* [71] both verified heartbeat detection algorithms on large datasets containing hundreds of thousands of heartbeats recorded in uncontrolled environments. Paalasmaa *et al.* used hierarchical clustering to first infer a heartbeat shape from the recordings, then beat-to-beat intervals were found by determining positions at which this template best fit the signal. The mean beat-to-beat interval error was 13 ms from 46 subjects in the clinic, home, single bed, double bed, and with two sensor types. Brueser *et al.* demonstrated robust estimation of heartbeats for 33 subjects of which 25 were insomniacs, with a mean beat-to-beat interval error of 0.78%. Their method used three short-time estimators combined using a Bayesian approach to continuously estimate interbeat intervals. Automatic template learning approaches were also presented by Brueser *et al.* in 2011 with low error [51].

Performance of HRV analysis using BCG measured on weighing scale-type load cell is evaluated in reference to the ECG during the resting and under each condition of Valsalva and postexercise sessions that induce cardiac autonomic rhythm changes [72]. Time domain, frequency domain, and nonlinear domain HRV parameters were evaluated on 15 healthy subjects to assess the cardiac autonomic modulation under each of these conditions. For all subjects and for all experimental sessions, HRV parameters calculated from BCG peak intervals are statistically not different from those obtained from the reference ECG. The results showed high performance with relative errors of 5.0–6.0% and strong correlation of 0.97–0.98 in average for these three states compared with the results from ECG peaks. The errors were relatively high in HRV parameters reflecting the high-frequency characteristics of heart rates such as HF, LF/HF in the spectral analysis, pNN50 in time-domain analysis, and SD1 in nonlinear analysis. This is considered to be caused by the inaccuracy in detecting peak from the less sharp J-peak of BCG compared to the R-peak in ECG. HRV estimates with BCG have also been compared to the PPG, and the correlation between the two was found to be high [73]. Preliminary work was recently presented by Brueser *et al.* for unsupervised HRV estimation from BCG signals [74].

B. Noise and Interference Reduction

Several sources of noise and interference can potentially corrupt BCG and SCG measurements taken using modern systems. These include sensor and circuit noise [75], motion artifacts [15], [21], [76], [77], and floor vibrations (for standing BCG measurements) [78].

Both BCG and SCG represent low-level signals that contain very low-frequency information—this can lead to problems with flicker (1/f) noise in the sensor interface circuit corrupting the measurements. Furthermore, many diseased subjects, and elderly subjects, have smaller signal amplitudes compared to the healthy young population [79]. The sensor and circuit noise were characterized and reduced for weighing-scale-based BCG systems using an ac-bridge amplifier approach [75]. This approach led to a SNR improvement of 6 dB.

For ambulatory and standing subjects, motion artifacts present the greatest potential obstacle to achieving reliable measurements. Unlike bed or chair systems, where the subject stays generally still for the measurement, postural sway, or ambulation can create unwanted peaks or distortion in the measured signals. Motion artifact detection for standing BCG measurements was accomplished using auxiliary sensors as noise references; then, gating the BCG signal based on the detection of excessive noise [76], [80]. In one study, the noise reference was an extra strain gauge added to the scale to detect postural sway [76]. In another study, the rms power of the electromyogram signal from the feet, indicating the presence of increased muscle contractions due to excessive movement, was used as a noise gate for the BCG [80]. Pandia *et al.* presented preliminary methods for cancelling motion artifacts in SCG signals from walking subjects, improving overall heartbeat detection [77]. Di Rienzo *et al.* used an automatic selection of movement-free data segments from daily recordings of SCG signals from ambulant subjects, followed by an ECG triggered ensemble averaging to reduce signal noise [21]. This enabled, for the first time, the assessment of systolic time interval profiles during normal daily living.

BCG measurements taken in a direction orthogonal to the plane of the floor can potentially be corrupted by floor vibrations—this can particularly pose a challenge for measurements taken on a vehicle [62] or plane [81]. Walter *et al.* instrumented the seat of a car with an EMFi mat to measure the BCG, aiming to use the information to monitor driver fitness [62]. However, with the engine turned on, the BCG was corrupted by vibration artifacts and rendered unusable. Inan *et al.* used an auxiliary sensor for vibration detection and adaptive noise cancellation to cancel floor vibration artifacts in the BCG measurement [78]. In this study, high-quality BCG measurements were successfully demonstrated from a subject standing on a bus with the engine turned on and idling. Additionally, it was observed that low-noise SCG waveforms could be obtained in a subject sitting in the metro, while a train was going by, with the above mentioned ensemble averaging approach [21].

C. Signal Modeling

Modeling of SCG and BCG provides a tool to better understand the genesis of waves in these signals and to simulate their morphological changes with different myocardial abnormalities. Modeling of BCG goes back to the early years of ballistocardiographic research [79].

In most BCG recording systems, the recording device is quite small compared to the human body and the platform on which it rests. It is also far away from the heart in most cases; thus,

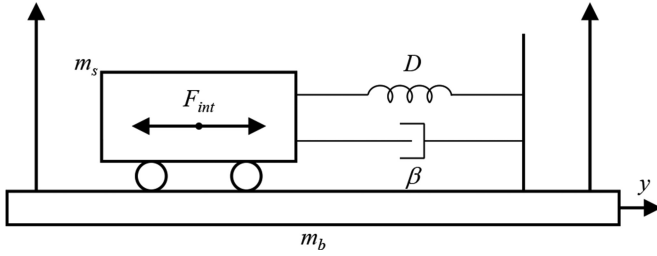


Fig. 3. Schematic showing the subject (with mass, m_s) and the BCG recording system (with mass, m_b) coupled by a spring dashpot system.

TABLE II
DESCRIPTIONS OF VARIABLES FOR SIGNAL MODELING

Variable	Description
F_{int}	Internal forces
β	Damping constant
y	Displacement or (in subscript) indicating head-to-foot direction
\dot{y}	Velocity
\ddot{y}	Acceleration
D	Spring constant
m_s	Mass of subject
m_b	Mass of recording device

the volume of the heart has been neglected in such models. The heart has been modeled like a point source providing the flow to the circulation system model [82]. Such a model is in accordance with the classical definition of BCG to be resulted through movement of center of gravity of the body and platform. On the contrary, in SCG the recording device (i.e., accelerometer) is near the heart and the volume of the heart cannot be neglected in any model dealing with SCG or any other precordial vibration signal. Thus, except for some preliminary efforts [83] SCG modeling has not been pursued by many researchers, probably because of the complications associated with such a model.

In ballistocardiographic research, one can study the events within human body that cause its movement in space, regardless of the recording device or to study the properties of instruments recording them and how their record relates to the movement originating them. Both of these two approaches are briefly introduced.

1) *Modeling the Recording Device:* During the early years of ballistocardiographic research, several different instruments were used to measure BCGs, from beds hanging from the ceiling [84] to tables strongly coupled to ground [1]. These instruments were giving different records from the same normal subjects. So, efforts were made to model the effect of these instruments on BCG morphology. Limiting ourselves to the head-foot direction the equation giving the components along the y -axis (Fig. 3, variables defined in Table II) reads:

$$(F_{int})_y - \beta \dot{y} - D y = (m_s + m_b) \ddot{y}. \quad (1)$$

After sorting and substituting $(F_{int})_y$ into $m_s \ddot{y}_c$ (where \ddot{y}_c is the acceleration of center of mass of body):

$$(m_s + m_b) \ddot{y} + \beta \dot{y} + D y = m_s \ddot{y}_c. \quad (2)$$

From the above equation, three different classic types of BCGs can be conceived based on the fact that which terms on the left side of the above equation can be neglected. The first is

$$(m_s + m_b) \ddot{y} = m_s \ddot{y}_c. \quad (3)$$

which means that the movement of bed and body is proportional to the movement of the center of gravity. A good approximation of this special case is when the ballistocardiograph is weakly coupled to the environment such as ultralow frequency BCG (ULF-BCG) systems.

The second type is when:

$$\dot{y} = \frac{m_s}{\beta} \ddot{y}_c \quad (4)$$

which represents Nickerson's low-frequency (LF) BCG and the third type is when:

$$y = \frac{m_s + m_b}{\beta} \ddot{y}_c \quad (5)$$

which refers to the situation when BCG is strongly coupled to its environment, which were categorized under high-frequency BCG (HF-BCG). In other words, when the resonance frequency of the BCG platform is much higher than heart frequency, then its displacement is proportional to the internal acceleration of body's center of gravity.

From this theoretical evaluation, it is clear that very different results will be obtained when one records any one aspect of motion such as displacement or acceleration from each of the three ideal types of ballistocardiographs [82]. However, there is a fourth category of classical BCGs, which are the direct body recordings based on AHA consensus paper on BCG terminology [85]. Direct body BCGs were always criticized for their inconsistencies [82].

2) *Modeling the Internal Forces:* Starr started on BCG modeling, where arteries were segmented into 3-cm long pieces and mass of blood in the aortic segment closest to the aortic valve was multiplied by acceleration, derived from cardiac ejection curve, to calculate force. This was repeated when the blood volume shifted to the next segment [82].

A more comprehensive model of human systemic arterial tree with distributed properties was constructed in early 1960s by Starr and Noordergraaf [82] and was improved later on by Westerhof *et al.* [86]. This model was based on the fact that, when using ULF systems, in which the body was free to move in space in the head-foot axis, it was observed that the body moved first footward and then headward during the cardiac cycle. This was explained as a movement to counteract the displacement of the blood mass, that, shortly after the onset of systole, is first driven headward out of the heart to distend the great vessels, and later footward, as the pulse wave spreads peripherally and blood accumulates at a great distance from the heart in the more peripheral vessels.

The model divided the arterial tree in 115 segments and calculated the position of the body's center of gravity in the longitudinal direction $y_c(t)$, as a function of time, by numerical integration of the products of the excess masses of each segment during the interval t , and the distance y_i between the centre of

each segment and the reference plane. Noordergraaf's model was successful in quantitatively predicting the amplitudes of ULF BCG waves and in giving an explanation for the origin of the main peaks. The model was verified on the data acquired from an astronaut in MIR station [87], where by using the longitudinal BCG recorded in space the model could be used to derive the aortic flow.

V. HUMAN SUBJECTS STUDIES WITH MODERN SYSTEMS

A. Correlation Studies With Healthy Subjects

Originally, BCG and SCG were proposed as diagnostic tools for the clinic—for example, a patient would lie on a Starr BCG table, the recording would be printed on a strip chart, and the physician would read the recording to make a diagnosis regarding the patient's cardiovascular health [1], [5]. However, the large intersubject variability in the signals hampered this approach, particularly given the limited tools available at that time for signal analysis. On the contrary, studies have shown that the intrasubject variability in the signals over serial measurements is actually low [15]—except in the presence of changing cardiovascular health. For this reason, in the past decade the BCG and SCG have been proposed as tools for monitoring changes in the same patient's health overtime. Then, the subject is his/her own control, and intersubject variability is no longer an obstacle.

To uncover the clinical relevance of BCG and SCG signal features, and to pave the way for future studies with clinical populations, several researchers conducted human subjects studies with a healthy population using modern instrumentation and analysis tools. These studies were mainly designed with a noninvasive protocol for altering the hemodynamics and timing intervals of the heart—such as exercise, Valsalva maneuver, whole-body tilt testing, or lower body negative pressure (LBNP)—then, comparing the changes in the BCG or SCG waveform to changes in a reference standard measurement, such as impedance cardiography (ICG) or Doppler ultrasound.

For both BCG and SCG signals the amplitude (or rms power) components have been shown to modulate with changes in left ventricular function—in particular, changes in stroke volume (SV) or cardiac output (CO). Castiglioni *et al.* measured clavicular SCG signals before and immediately after exercise and compared the percent changes in the peak-to-peak amplitude of the SCG to changes in CO as measured by the finometer model flow method, finding a strong correlation for four data points taken from four subjects [24]. Inan *et al.* further demonstrated that the changes in rms power resulting from exercise, measured during 10 min of recovery time, were strongly correlated to changes in CO measured by Doppler ultrasound for 275 data points taken from nine subjects [88]. Tavakolian *et al.* trained a neural network to estimate SV from SCG parameters and tested this classifier on a separate testing dataset, finding an average correlation coefficient of 0.61, and Bland–Altman agreement limits (95% confidence) of +7.4mL, −7.6mL for 4900 heartbeats analyzed from eight participants [16]. It is important to note that these error bands are larger than what would be needed for absolute volume estimation using the SCG; however, this may be of interest for future research.

Many researchers have also examined the time intervals both within the signals themselves, and between BCG / SCG signal features and other physiological measurements (e.g., ECG or PPG), to form a relationship between these timing intervals to more well-known parameters [e.g., preejection period (PEP), pulse transit time (PTT), or left ventricular ejection time (LVET)]. The time interval between the ECG R-wave peak and the BCG J-wave peak has been proposed as a surrogate for the PEP—a measure of the IVC period of the heart and an index of cardiac contractility [30], [89]. These authors used the Valsalva maneuver and/or whole body tilt testing to modulate the PEP by changing the autonomic balance between parasympathetic and sympathetic drive, and compared the R-J interval to the PEP measured using ICG. Etemadi *et al.* demonstrated a strong correlation ($R^2 = 0.86$) between the R-J interval and the PEP for 2126 heartbeats across ten subjects performing the Valsalva maneuver [89]. He *et al.* showed similar results for one example subject with both the Valsalva maneuver and whole-body tilt testing [30]. Tavakolian *et al.* proposed the interval between the ECG Q-wave and the SCG AO-point as a surrogate for PEP, and found strong correlation between this interval and PEP measurement using ICG and Doppler ultrasound in 25 subjects [16].

Researchers have also attempted to extract data from the BCG relating to blood pressure (BP), leveraging the known relationship between pulse wave velocity estimated using PTT, and Pinheiro *et al.* suggested the use of BCG and PPG for PTT estimation [90]. Shin *et al.* compared the R-J interval of the BCG, modulated using the Valsalva maneuver, to beat-by-beat systolic BP (SBP) measurements taken using the Finapres system, finding a strong correlation [39]. Nevertheless, Casanella *et al.* found that, in case of hemodynamic changes induced by paced respiration, this correlation between R-J interval and SBP was dependent on the subject and was not always observed [91]. Winokur *et al.* found, for one example subject, that the time interval between the BCG and the PPG signal, both measured at the ear, were correlated to PTT, and could thus be used to estimate BP [31].

Another important interval is the duration of systolic ejection, the LVET, as it provides an indication of what percentage of the cardiac cycle is being devoted to ejection compared to filling. Tavakolian *et al.* used LBNP to simulate hemorrhage, and found that LVET measurements taken using SCG were significantly different at various stages of LBNP, and correlates with the LBNP levels ($R = 0.90$) for 32 subjects [92]. Di Rienzo *et al.* found that with exercise LVET changes measured using wearable SCG are in line with the changes reported in the literature and obtained by traditional laboratory techniques [21], [93].

B. Clinical Findings From Patients With Cardiovascular Disease

Modern ballistocardiography and seismocardiography systems may be capable of monitoring slow, longitudinal changes in cardiac function associated with a number of cardiovascular diseases. Timely noninvasive detection of subtle changes in cardiac pathophysiology may one day enable daily drug dosage adjustments, thus reducing costly and morbid rehospitalizations

[94]. At this moment, the feasibility of this approach is investigated by the ongoing LAPTOP-HF study which, however, uses an implantable right atrial pressure sensor coupled to a mobile device that allows daily automatic dosage adjustment [95].

Fortunately, the basis for the SCG's clinical utility was begun in 1990 with the initial use of high sensitivity, LF accelerometers to measure precordial vibrations [96]. Significant features of the SCG waveform were identified and associated with key events in the cardiac cycle [17]. This allowed the accurate measurement of these features (e.g., ACs and MOs) using one sensor, greatly simplifying the calculation of CTIs.

A large body of work exists on the utility and efficacy of CTIs [97], [98]. This knowledge combined with the ability to make accurate, repeatable quantitative measurements using the SCG resulted in the ability to conduct clinically relevant cross-sectional studies. Subsequently, clinical studies were undertaken to determine if the SCG could be used to identify changes in the SCG waveform resulting from myocardial ischemia [99].

The SCG's clinical utility in enhancing the diagnostic outcome of a graded exercise stress test was first shown in [100]. A large multicenter study demonstrated that when the combined results of the ECG and SCG were used, the predictive accuracy of detecting physiologically significant coronary artery disease was increased significantly over the results of the ECG alone [7].

The introduction in the early 1990s of lightweight (<25g) accelerometers, whose working range extended below 1 Hz, made possible other clinical settings for the SCG. The SCG as a magnetic-field-compatible alternative to the electrocardiogram for cardiac stress monitoring [101] was made possible using a newly introduced light weight piezoelectric accelerometer (336C, PCB Piezotronics, Depew, NY, USA).

The SCG was used to measure CTI's during atrial, ventricular, and biventricular pacing, as compared to normals [102]. One of the studies objectives was to determine the utility of the SCG in cardiac resynchronization therapy (CRT). This study was the first to use 3 SCG traces for analysis, i.e., one accelerometer was placed on the xiphoid process, a second over the apex at the fourth intercostal, and a third on the right carotid pulse.

In 1994, the SCG was used to make accurate longitudinal measurements in a study of the effects of elgodipine on cardiac hemodynamics [103]. In a sports medicine application, exercise capacity was evaluated using the SCG [104]. A more extensive review of the SCG is available in [105].

As a note of interest, the combined patient population of the myocardial ischemia studies [7], [100] is close to 2000 and consists of both healthy and disease subjects. All the raw data were recorded with the same instrumentation (SCG 2000, SeisMed Instruments, Minneapolis, MN, USA) associated with these datasets are complete patient demographics. A project is underway to make the raw data available on the PhysioNet website for study by interested researchers [105].

More recent findings with BCG and SCG further support that the signals have great potential in allowing proactive cardiac disease management without a costly implantable device. However, despite stated clinical and/or physiologic motivations, the overwhelming majority of modern BCG/SCG findings continue to be from healthy subjects [106]–[108]. Notable exceptions in-

clude a bed-mounted BCG system for automated detection of atrial fibrillation [109], the observation of reduced signal amplitude in the setting of premature atrial or ventricular contractions [15], and the reduction of signal consistency in heart failure patients concordant with worsening clinical outcome [110].

One particular subset of patients is particularly well suited for study using cardiomechanical signals, those undergoing CRT. CRT patients have abnormal cardiac conduction causing in a significant delay between the pumping action of the various chambers of the heart. CRT involves precisely adjusting the timing of a multichamber pacemaker to reduce or remove these delays. Such timing is difficult to ascertain using available technologies, spawning the field of "CRT optimization." Researchers recently demonstrated the benefits of intracardiac acceleration monitoring in performing CRT optimization [111], a finding preliminarily corroborated by BCG findings as well [8].

C. 3-D Ballistocardiography and Microgravity Studies

As the sections on instrumentation earlier in this review have indicated, measurements of BCG (in particular) are constrained by the coupling of the body to the ground, a direct result of the influence of gravity. As such, full 3-D recordings of the BCG are difficult in the terrestrial environment, and much of the focus has been on accelerations in the coronal plane (the XY plane as defined in the section on measurement axes).

Given this limitation, it is therefore not surprising that the idea of measuring the BCG in a subject in free-fall (weightlessness, zero-G, microgravity) was an obvious target of investigation. The first such experiment was performed in the 1960s in parabolic flight, with the subject strapped into a "tub," which was itself instrumented to record the BCG [9]. Despite the limited periods of microgravity available (typically ~20 s) and the subject restraints, recordings of good quality were obtained.

Spaceflight represents the other obvious environment in which the "true" 3-D BCG can be recorded. The earliest recordings were made by the Soviets on Saluyt-6 [10] and consisted of a series of five recordings were performed in two crew members of a long duration mission on days 46, 71, 98, 133, and 175. A piezoelectric sensor, attached close to the center of mass, recorded ballistic forces in the feet-to-head axis during breath holding experiments. Individual changes were seen during the mission with maximum amplitude of the IJ wave occurring on day 133. Measurements were also made during the Spacelab-1 mission aboard the Space Shuttle in 1983 [112]. These experiments were conducted in two subjects at two occasions during this short duration spaceflight and showed an increase of the overall systolic accelerations along the longitudinal axis in microgravity.

Perhaps the best-analyzed dataset of the BCG in spaceflight came from measurements made during the Spacelab D-2 mission in 1993. During that flight, extra time became available (due to an extension of the overall mission length), and an experiment was hastily conceived, approved, implemented, and performed to measure 3-D BCG in a free-floating subject. Parenthetically, this may be one of the fastest spaceflight experiments ever developed with the time from concept, to collection of the data



Fig. 4. Subject in D-2 shown wearing the snugly-fitting suit incorporating a respiratory inductance plethysmograph and ECG. Photo Credit: NASA.

816 (including approval of an institutional review board) was only
 817 4–5 days, surely some sort of record. The experiment utilized
 818 data from a free-floating subject instrumented with an ECG
 819 and wearing a snugly fitting suit that measured respiratory
 820 motion using an impedance plethysmograph (see Fig. 4). This
 821 instrumentation was a part of the Anthrock series of human
 822 studies managed by the European Space Agency. The second
 823 crucial piece of instrumentation was a set of high-fidelity tri-
 824 axial accelerometer that were attached to the vehicle and used
 825 for measuring the accelerations imparted by crew activity in
 826 the Spacelab. The sensor package was detached from the ve-
 827 hicle and taped to the lumbar region of the subject, near to
 828 the (presumed) center of mass. Data were then recorded as
 829 the subject remained stationary and free floated in the center
 830 of the Spacelab, providing a continuous recording, free of in-
 831 terruptions of 146 s. In order to synchronize the two separate
 832 data streams, collisions with the Spacelab structure, which dis-
 833 rupted signals in both data streams, were used as posthoc event
 834 source [11].

835 The data from the D-2 study and some subsequent studies
 836 provided valuable insight into several aspects of the BCG. In
 837 particular there were four major conclusions derived from this
 838 dataset.

- 839 1) Lung volume greatly influences the accelerations
 840 recorded, especially in the longitudinal (head-to-foot)
 841 body axis (see Fig. 5), with the implication being that
 842 there is better coupling between the heart and the body in
 843 the longitudinal axis at higher lung volumes [11]. Inter-
 844 estingly, the actual direction of respiratory motion (mid
 845 inspiration versus mid expiration) had only minimal in-
 846 fluence of the BCG.
- 847 2) Data derived from short periods of microgravity in
 848 parabolic flight are largely equivalent to data obtained
 849 in sustained microgravity [113].
- 850 3) The BCG has a plane of symmetry that is primarily sagi-
 851 tal. This suggests that 2-D recordings performed in a
 852 supine subject (i.e., coronal recordings) fail to capture
 853 a significant portion of the effect of the blood ejection
 854 to the body, complicating their interpretation [113].

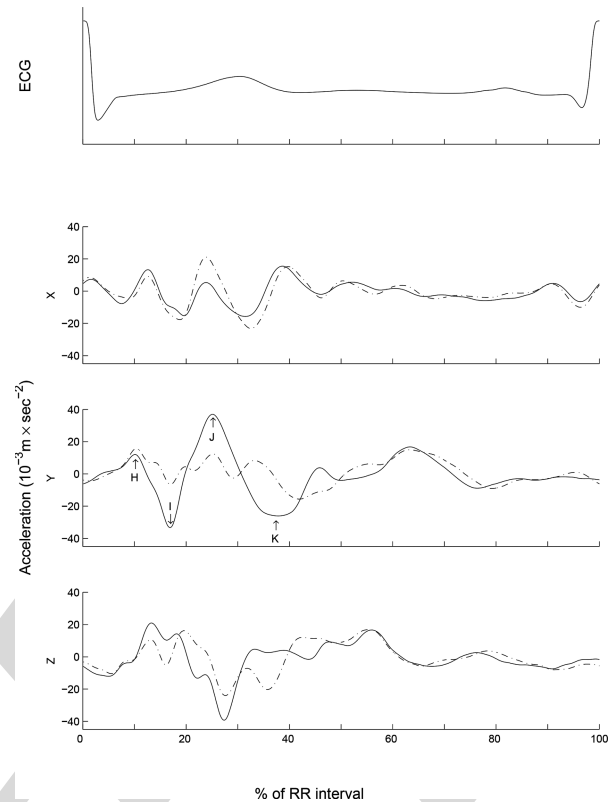


Fig. 5. The 3-D BCG recorded in spaceflight in a free-floating subject, at the end of a normal expiration (dashed lines, functional residual capacity, FRC), and at the end of a normal inspiration (solid lines, FRC + tidal volume). From [11].

- 4) The accelerations that are recording in a 2-D system are only modestly correlated with the true 3-D accelerations that actually occur, again complicating their interpretation [113].

BCG flight experiments were also an integral part of the Russian cardiovascular research program for the orbital station MIR. BCG along the head-to-foot direction was measured in three crew members during the second MIR mission in 1988 and compared to SCG recordings. Significant changes of the BCG amplitudes (HI, IJ, JK) during the long-term flight were described together with large inter individual differences. The first true 3-D-BCG recordings were made during the sixth MIR mission in 1990 in two crew members on flight days 56 and 110. Three new piezoelectric sensors were used placed in perpendicular planes in a small cylindrical box with a diameter of 40 mm and a height of 20 mm. The sensitivity of the sensor was 20 mV/m/s². The sensor was placed between the scapulae using rubber belts and a metallic plate. The special amplifier (BCG-3) was connected to the recording unit “Gamma-1,” and the data were transmitted telemetrically to the ground station. In summary, no dramatic changes in the vector sum were detected. Maximum forces ranged from 5.85 to 10.18 N. However, profound individual changes of the shape, amplitude, and timing of the BCG, especially in the lateral and dorso-ventral plane have been found. Finally, combined BCG and SCG measurements have been made every month in space during the 14 months space flight of Valeri Poljakov,

882 15th to 17th MIR missions (Russian–Austrian flight experiment
883 “Pulstrans”) [114].

884 VI. STANDARDS AND OPEN ISSUES

885 A. Need For a Standardization

886 From the analysis of the literature, it appears that important
887 methodological aspects concerning BCG and SCG analysis are
888 still characterized by a certain level of ambiguity. These include

889 1) *Definitions of BCG and SCG Signals*: In the literature, the
890 definition of BCG and SCG is not univocal and the “BCG” term
891 is even sometimes used for SCG signals.

892 2) *Nomenclature*: Since BCG and SCG waveforms are
893 mostly different (although they might have some common fea-
894 tures to be investigated) it is reasonable to use a specific nomen-
895 clature for defining peaks and valleys of each signal. The preva-
896 lent annotation for BCG was proposed by Starr *et al.* [1], for
897 SCG by Crow *et al.* [17]. However, there are some disagree-
898 ments on these annotations, and in some instances, SCG peaks
899 are termed with the BCG annotation.

900 3) *Indication of Site of Measurement, Characteristics of sen-
901 sor, Sensor Axis Orientation*: These pieces of information are
902 crucial for data comparison and interpretation, but unfortunately
903 are not invariably reported in scientific communications.

904 A standardization or at least a common position on the above
905 issues would greatly facilitate the understanding and comparison
906 of published results, the exchange of data, and the design of new
907 experimental protocols in this area.

908 B. Open Issues

909 A number of open issues remain to be addressed in this field to
910 improve the understanding and applicability of BCG and SCG
911 signals. Hereafter, we provide just a short list of these issues.

- 912 1) The biological meaning of BCG and SCG deflections not
913 yet annotated and their clinical relevance.
- 914 2) Possible common features of the BCG and SCG signals.
- 915 3) Further parameters derivable from the analysis of the BCG
916 and SCG 3-D vectors.
- 917 4) Effects of respiration, posture, right ventricle, and sensor
918 adherence on the signal waveform/quality.
- 919 5) How to facilitate the use of these signals in clinical prac-
920 tice?
- 921 6) Reference values for healthy and diseased subjects for
922 both types of signals, and for a wide range of body
923 types/sizes, and ages.

924 VII. CONCLUSION AND AREAS FOR FUTURE INVESTIGATION

925 The recent advances in the BCG and SCG field indicate the
926 strong potential of these measurements to address wide vari-
927 ety of clinical needs, in particular monitoring or trending the
928 cardiomechanical health of patients outside of the clinic. Both
929 BCG and SCG measurements can be taken using inexpensive
930 and unobtrusive sensors, making them ideally suited, for exam-
931 ple, for home monitoring of chronic diseases. Nevertheless, to
932 maximize our ability to interpret these signals, the physiological

origins of both signals must be studied further and elucidated. 933
Furthermore, there is a need to be able to map each measure- 934
ment modality to another using cardiovascular and mechanical 935
modeling of the body, such that any BCG or SCG waveform 936
amplitude, timing, or morphology measured using one modal- 937
ity can be translated quantitatively to another. For example, 938
if a bed-based recording in the dorso–ventral axis yielded a 939
peak BCG J-wave amplitude of 2 N, system modeling tools are 940
needed to compare this to a corresponding J-wave amplitude 941
measured using a weighing scale. Finally, an extensive, open 942
database of BCG and SCG signals, processing tools, and even 943
microprocessor code needs to be made available to massively 944
expand the capability of researchers around the world to inves- 945
tigate these signals, use them in their own settings, and grow the 946
field from a niche into an established technique, routinely used 947
in clinical practice. 948

REFERENCES 949

- [1] I. Starr, A. J. Rawson, H. A. Schroeder *et al.*, “Studies on the estimation 950
of cardiac output in man, and of abnormalities in cardiac function, from 951
the heart’s recoil and the blood’s impacts; the ballistocardiogram,” *Amer.* 952
J. Physiol., vol. 127, pp. 1–28, 1939. 953
- [2] B. S. Bozhenko, “Seismocardiography—a new method in the study 954
of functional conditions of the heart [Article in Russian],” *Ter Arkh.*, 955
vol. 33, pp. 55–64, 1961. 956
- [3] J. W. Gordon, “Certain molar movements of the human body produced 957
by the circulation of the blood,” *J. Anat. Physiol.*, vol. 11, pp. 533–536, 958
1877. 959
- [4] D. M. Salerno and J. Zanetti, “Seismocardiography for monitoring 960
changes in left ventricular function during ischemia,” *Chest J.*, vol. 100, 961
pp. 991–993, 1991. 962
- [5] I. Starr and F. C. Wood, “Studies with the ballistocardiograph in acute 963
cardiac infarction and chronic angina pectoris,” *Amer. Heart J.*, vol. 25, 964
pp. 81–101, 1943. 965
- [6] H. Mandelbaum and R. A. Mandelbaum, “Studies utilizing the portable 966
electromagnetic ballistocardiograph: IV. The clinical significance of se- 967
rial ballistocardiograms following acute myocardial infarction,” *Circu-* 968
lation, vol. 7, pp. 910–915, 1953. 969
- [7] R. A. Wilson, V. S. Bamrah, J. J. Lindsay *et al.*, “Diagnostic accu- 970
racy of seismocardiography compared with electrocardiography for the 971
anatomic and physiologic diagnosis of coronary artery disease during 972
exercise testing,” *Amer. J. Cardiol.*, vol. 71, pp. 536–545, 1993. 973
- [8] L. Giovangrandi, O. T. Inan, R. M. Wiard *et al.*, “Ballistocardiography: 974
A method worth revisiting,” in *Proc. IEEE Annu. Int. Conf. Eng. Med.* 975
Biol. Soc., 2011, pp. 4279–4282. 976
- [9] W. C. Hixson and D. E. Beischer, “Biotelemetry of the triaxial ballisto- 977
cardiogram and electrocardiogram in a weightless environment,” Naval 978
School Aviat. Med., Pensacola, FL, USA, 1964. 979
- [10] R. M. Baevsky and I. I. Funtova, “Ballistocardiographic examinations of 980
the saljut-6 fourth expedition crew members,” *Komsich Biologiya Aviak* 981
Medit, vol. 16, pp. 34–37, 1982. 982
- [11] G. K. Prisk, S. Verhaeghe, D. Padeken *et al.*, “Three-dimensional ballis- 983
tocardiography and respiratory motion in sustained microgravity,” *Aviat.* 984
Space Environ. Med., vol. 72, pp. 1067–1074, 2001. 985
- [12] P. F. Migeotte, S. De Ridder, J. Tank *et al.*, “Three dimensional ballisto- 986
and seismo-cardiography: HIJ wave amplitudes are poorly correlated to 987
maximal systolic force vector,” in *Proc. IEEE Annu. Int. Conf. Eng. Med.* 988
Biol. Soc., 2012, pp. 5046–5049. 989
- [13] R. M. Wiard, H. J. Kim, C. A. Figueroa *et al.*, “Estimation of central aortic 990
forces in the ballistocardiogram under rest and exercise conditions,” in 991
Proc. IEEE Annu. Int. Conf. Eng. Med. Biol. Soc., 2009, pp. 2831–2834. 992
- [14] M. Di Rienzo, P. Meriggi, F. Rizzo *et al.*, “A wearable system for the 993
seismocardiogram assessment in daily life conditions,” in *Proc. IEEE* 994
Annu. Int. Conf. Eng. Med. Biol. Soc., 2011, pp. 4263–4266. 995
- [15] O. T. Inan, M. Etemadi, R. M. Wiard *et al.*, “Robust ballistocardiogram 996
acquisition for home monitoring,” *Physiol. Meas.*, vol. 30, pp. 169–185, 997
2009. 998

- 999 [16] K. Tavakolian, "Characterization and analysis of seismocardiogram for
1000 estimation of hemodynamic parameters," Ph.D. dissertation, Dept. Appl.
1001 Sci, School Eng. Sci., Simon Fraser Univ., Burnaby, BC, Canada, 2010.
- 1002 [17] R. S. Crow, P. Hannan, D. Jacobs *et al.*, "Relationship between seismo-
1003 cardiogram and echocardiogram for the events in the cardiac cycle,"
1004 *Amer. J. Noninvasive Cardiol.*, vol. 8, pp. 39–46, 1994.
- 1005 [18] O. T. Inan, M. Etemadi, R. M. Wiard *et al.*, "Novel methods for esti-
1006 mating the ballistocardiogram signal using a simultaneously acquired
1007 electrocardiogram," in *Proc. IEEE Annu. Int. Conf. Eng. Med. Biol. Soc.*,
1008 2009, pp. 5334–5347.
- 1009 [19] K. Pandia, O. T. Inan, G. T. A. Kovacs *et al.*, "Extracting respiratory
1010 information from seismocardiogram signals acquired on the chest using a
1011 miniature accelerometer," *Physiol. Meas.*, vol. 33, pp. 1643–1660, 2012.
- 1012 [20] Y. Chuo and B. Kaminska, "Sensor layer of a multiparameter single-point
1013 integrated system," *IEEE Trans. Biomed. Circuits Syst.*, vol. 3, no. 4,
1014 pp. 229–240, Aug. 2009.
- 1015 [21] M. D. Rienzo, E. Vaini, P. Castiglioni *et al.*, "Wearable seismocardiogra-
1016 phy: Towards a beat-by-beat assessment of cardiac mechanics in ambu-
1017 lant subjects," *Autonomic Neurosci.*, vol. 178, pp. 50–59, 2013.
- 1018 [22] B. Ngai, K. Tavakolian, A. Akhbardeh *et al.*, "Comparative analysis
1019 of seismocardiogram waves with the ultra-low frequency ballistocardi-
1020 ogram," in *Proc. IEEE Annu. Int. Conf. Eng. Med. Biol. Soc.*, 2009,
1021 pp. 2851–2854.
- 1022 [23] M. J. T. Paukkunen, M. T. Linnavuo, and R. E. Sepponen, "A portable
1023 measurement system for the superior-inferior axis of the seismocardi-
1024 ogram," *J. Bioeng. Biomed. Sci.*, vol. 3, 2013.
- 1025 [24] P. Castiglioni, A. Faini, G. Parati *et al.*, "Wearable seismocardiography,"
1026 in *Proc. IEEE 29th Annu. Int. Conf. Eng. Med. Biol. Soc.*, 2007, pp. 3954–
1027 3957.
- 1028 [25] Y. Chuo, M. Marzencki, B. Hung *et al.*, "Mechanically flexible wireless
1029 multisensor platform for human physical activity and vitals monitoring,"
1030 *IEEE Trans. Biomed. Circuits Syst.*, vol. 4, no. 5, pp. 281–294, Oct. 2010.
- 1031 [26] R. M. Baevsky, I. I. Funtova, A. Diedrich *et al.*, "Autonomic function
1032 testing aboard the ISS using 'PNEUMOCARD'," *Acta Astronautica*, vol.
1033 65, pp. 930–932, 2009.
- 1034 [27] P. F. Migeotte, Q. Deliere, J. Tank *et al.*, "3D-ballistocardiography in
1035 microgravity: Comparison with ground based recordings," presented at the
1036 *IEEE Eng. Med. Biol. Soc.*, Osaka, Japan, 2013, pp. 7012–7016.
- 1037 [28] E. Luchitskaya, Q. Deliere, A. Diedrich *et al.*, "Timing and source of the
1038 maximum of the transthoracic impedance cardiogram (dZ/dt) in relation
1039 to the H-I-J complex of the longitudinal ballistocardiogram under gravity
1040 and microgravity conditions," presented at the *IEEE Eng. Med. Biol. Soc.*,
1041 Osaka, Japan, 2013, pp. 7294–7297.
- 1042 [29] Q. Deliere, P. F. Migeotte, X. Neyt *et al.*, "Cardiovascular changes in
1043 parabolic flights assessed by ballistocardiography," presented at the *IEEE
1044 Eng. Med. Biol. Soc.*, Osaka, Japan, 2013, pp. 3801–3804.
- 1045 [30] D. D. He, E. S. Winokur, and C. G. Sodini, "A continuous, wearable, and
1046 wireless heart monitor using head ballistocardiogram (BCG) and head
1047 electrocardiogram (ECG)," in *Proc. IEEE Annu. Int. Conf. Eng. Med.
1048 Biol. Soc.*, 2011, pp. 4729–4732.
- 1049 [31] E. S. Winokur, D. D. He, and C. G. Sodini, "A wearable vital signs
1050 monitor at the ear for continuous heart rate and pulse transit time mea-
1051 surements," in *Proc. IEEE Annu. Int. Conf. Eng. Med. Biol. Soc.*, 2012,
1052 pp. 2724–2727.
- 1053 [32] E. Hyun, S. Noh, C. Yoon *et al.*, "Patch type integrated sensor system
1054 for measuring electrical and mechanical cardiac activities," presented
1055 at the *IEEE Sensors Applications Symposium (SAS)*, Queenstown, New
1056 Zealand, 2014.
- 1057 [33] G. Balakrishnan, F. Durand, and J. Guttag, "Detecting pulse from head
1058 motions in video," in *Proc. IEEE Conf. Comput. Vis. Pattern Recog.*,
1059 2013, pp. 3430–3437.
- 1060 [34] J. Williams. 1990, *Bridge Circuits: Marrying Gain and Balance. Linear
1061 Technology Application Note 43.*
- 1062 [35] S. I. Chaudhry, J. A. Mattera, J. P. Curtis, *et al.*, "Telemonitoring in
1063 patients with heart failure," *N. Engl. J. Med.*, vol. 363, pp. 2301–2309,
1064 2010.
- 1065 [36] S. I. Chaudhry, Y. Wang, J. Concato *et al.*, "Patterns of weight
1066 change preceding hospitalization for heart failure," *Circulation*, vol. 116,
1067 pp. 1549–1554, 2007.
- 1068 [37] J. Gomez-Clapers, A. Serra-Rocamora, R. Casanella *et al.*, "Uncertainty
1069 factors in time-interval measurements in ballistocardiography," in *Proc.
1070 19th IMEKO TC-4 Symp. 17th IWADC Workshop Adv. Instrum. Sens.
1071 Interoperability*, Barcelona, Spain, 2013, pp. 395–399.
- 1072 [38] R. Gonzalez-Landaeta, O. Casas, and R. Pallas-Areny, "Heart rate
1073 detection from an electronic weighing scale," *Phys. Meas.*, vol. 29,
1074 pp. 979–988, 2008.
- [39] J. H. Shin, K. M. Lee, and K. S. Park, "Non-constrained monitoring
1075 of systolic blood pressure on a weighing scale," *Phys. Meas.*, vol. 30,
1076 pp. 679–693, 2009.
- [40] J. Alihanka, K. Vaahtoranta, and I. Saarikivi, "A new method for long-
1078 term monitoring of the ballistocardiogram, heart rate, and respiration,"
1079 *Amer. J. Physiol.*, vol. 240, pp. R384–R392, 1981.
- [41] Y. Chee, J. Han, and K. S. Park, "Air mattress sensor system with bal-
1081 ancing tube for unconstrained measurement of respiration and heart beat
1082 movements," *Phys. Meas.*, vol. 26, pp. 413–422, 2005.
- [42] D. C. Mack, J. T. Patrie, P. M. Suratt *et al.*, "Development and preliminary
1084 validation of heart rate and breathing rate detection using a passive,
1085 ballistocardiography-based sleep monitoring system," *IEEE Trans Inf.
1086 Technol. Biomed.*, vol. 13, no. 1, pp. 111–120, Jan. 2009.
- [43] A. Vehkaoja, S. Rajala, P. Kumpulainen *et al.*, "Correlation approach for
1088 the detection of the heartbeat intervals using force sensors placed under
1089 the bed posts," *J. Med. Eng. Technol.*, vol. 37, pp. 327–333, 2013.
- [44] B. H. Choi, G. S. Chung, J.-S. Lee *et al.*, "Slow-wave sleep estimation
1091 on a load cell installed bed: A non-constrained method," *Phys. Meas.*,
1092 vol. 30, pp. 1163–1170, 2009.
- [45] Y. Zhu, H. Zhang, M. Jayachandran *et al.*, "Ballistocardiography with
1094 fiber optic sensor in headrest position: A feasibility study and a new
1095 processing algorithm," in *Proc. 35th IEEE Annu. Int. Conf. Eng. Med.
1096 Biol. Soc.*, 2013, pp. 5203–5206.
- [46] S. Sprager and D. Zazula, "Heartbeat and respiration detection from
1098 optical interferometric signals by using a multimethod approach," *IEEE
1099 Trans. Biomed. Eng.*, vol. 59, no. 10, pp. 2922–9, Oct. 2012.
- [47] L. Dziuda and F. Skibniewski, "Monitoring respiration and cardiac activ-
1101 ity using fiber Bragg grating-based sensor," *IEEE Trans. Biomed. Eng.*,
1102 vol. 59, no. 7, pp. 1934–42, Jul. 2012.
- [48] J. M. Kortelainen and J. Virkkala, "FFT averaging of multichannel BCG
1104 signals from bed mattress sensor to improve estimation of heart beat
1105 interval," in *Proc. IEEE 29th Annu. Int. Conf. Eng. Med. Biol. Soc.*,
1106 2007, pp. 6685–6688.
- [49] J. Paalasmaa, M. Waris, H. Toivonen *et al.*, "Unobtrusive online moni-
1108 toring of sleep at home," in *Proc. IEEE Annu. Int. Conf. Eng. Med. Biol.
1109 Soc.*, 2012, pp. 3784–3788.
- [50] F. Wang, M. Tanaka, and S. Chonan, "Development of a PVDF piezopoly-
1111 mer sensor for unconstrained in-sleep cardiorespiratory monitoring,"
1112 *J. Intell. Mater. Syst. Struct.*, vol. 14, pp. 185–190, 2003.
- [51] C. Bruser, K. Stadlthanner, S. De Waele *et al.*, "Adaptive beat-to-beat
1114 heart rate estimation in ballistocardiograms," *IEEE Trans Inf. Technol.
1115 Biomed.*, vol. 15, no. 5, pp. 778–786, Sep. 2011.
- [52] K. Watanabe, T. Watanabe, H. Watanabe *et al.*, "Noninvasive measure-
1117 ment of heartbeat, respiration, snoring and body movements of a subject
1118 in bed via a pneumatic method," *IEEE Trans. Biomed. Eng.*, vol. 52,
1119 no. 12, pp. 2100–07, Dec. 2005.
- [53] X. Zhu, W. Chen, T. Nemoto *et al.*, "Real-time monitoring of respiration
1121 rhythm and pulse rate during sleep," *IEEE Trans. Biomed. Eng.*, vol. 53,
1122 no. 12, pp. 2553–63, Dec. 2006.
- [54] J. Kortelainen, M. V. Gils, and J. Parkka, "Multichannel bed pressure
1124 sensor for sleep monitoring," presented at the *Comput. Cardiol. Conf.*,
1125 Kraków, Poland, 2012.
- [55] C. Brueser, A. Kerekes, S. Winter *et al.*, "Multi-channel optical sensor-
1127 array for measuring ballistocardiograms and respiratory activity in bed,"
1128 presented at the *IEEE 34th Ann. Int. Conf. Eng. Med. Biol. Soc.*, San
1129 Diego, CA, USA, 2012.
- [56] T. Watanabe and K. Watanabe, "Noncontact method for sleep stage esti-
1131 mation," *IEEE Trans. Biomed. Eng.*, vol. 51, no. 10, pp. 1735–1748, Oct.
1132 2004.
- [57] D. W. Jung, S. H. Hwang, H. N. Yoon *et al.*, "Nocturnal awakening
1134 and sleep efficiency estimation using unobtrusively measured ballisto-
1135 cardiogram," *IEEE Trans. Biomed. Eng.*, vol. 61, no. 1, pp. 131–138, Jan.
1136 2014.
- [58] J. M. Kortelainen, M. O. Mendez, A. M. Bianchi *et al.*, "Sleep staging
1138 based on signals acquired through bed sensor," *IEEE Trans Inf. Technol.
1139 Biomed.*, vol. 14, no. 3, pp. 776–785, May 2010.
- [59] M. Migliorini, A. M. Bianchi, Nistico *et al.*, "Automatic sleep staging
1141 based on ballistocardiographic signals recorded through bed sensors," in
1142 *Proc. IEEE Annu. Int. Conf. Eng. Med. Biol. Soc.*, 2010, pp. 3273–3276.
- [60] K. Tanida, M. Shibata, and M. M. Heitkemper, "Sleep stage assessment
1144 using power spectral indices of heart rate variability with a simple algo-
1145 rithm: limitations clarified from preliminary study," *Biol. Res. Nursing*,
1146 vol. 15, pp. 264–272, 2013.
- [61] T. Koivistoinen, S. Junnila, A. Varri *et al.*, "A new method for measuring
1148 the ballistocardiogram using EMFi sensors in a normal chair," in *Proc.
1149 IEEE 26th Annu. Int. Conf. Eng. Med. Biol. Soc.*, 2004, pp. 2026–2029.

- [62] M. Walter, B. Eilebrecht, T. Wartzek *et al.*, "The smart car seat: Personalized monitoring of vital signs in automotive applications," *Pers. Ubiquitous Comput.*, vol. 15, pp. 707–715, 2011.
- [63] Y. Lim, K. Hong, K. Kim *et al.*, "Monitoring physiological signals using noninvasive sensors installed in daily life equipment," *Biomed. Eng. Lett.*, vol. 1, pp. 11–20, 2011.
- [64] B. H. Jansen, B. H. Larson, and K. Shankar, "Monitoring of the ballistocardiogram with the static charge sensitive bed," *IEEE Trans. Biomed. Eng.*, vol. 38, no. 8, pp. 748–751, Aug. 1991.
- [65] J. H. Shin, B. H. Choi, Y. G. Lim *et al.*, "Automatic ballistocardiogram (BCG) beat detection using a template matching approach," in *Proc. IEEE 30th Annu. Int. Conf. Eng. Med. Biol. Soc.*, 2008, pp. 1144–1146.
- [66] D. Friedrich, X. L. Aubert, H. Fuhr *et al.*, "Heart rate estimation on a beat-to-beat basis via ballistocardiography—a hybrid approach," presented at the *IEEE 32nd Annu. Int. Conf. Eng. Med. Biol. Soc.*, Buenos Aires, Argentina, 2010.
- [67] S. Sprager and D. Zazula, "Optimization of heartbeat detection in fiberoptic unobtrusive measurements by using maximum a posteriori probability estimation," *IEEE J. Biomed. Health Informat.*, vol. 18, no. 4, pp. 1161–1168, Jul. 2014.
- [68] W. Xu, W. A. Sandham, A. C. Fisher *et al.*, "Detection of the seismocardiogram W complex based on multiscale edges," presented at the *18th Annu. Int. Conf. IEEE EMBS (EMBC)*, Amsterdam, The Netherlands, 1996.
- [69] C. Bruser, J. M. Kortelainen, S. Winter *et al.*, "Improvement of force-sensor-based heart rate estimation using multi-channel data fusion," *IEEE J. Biomed. Health Informat.*, 2014, to be published.
- [70] J. Paalasmaa, H. Toivonen, and M. Partinen, "Adaptive heartbeat modelling for beat-to-beat heart rate measurement in ballistocardiograms," *IEEE J. Biomed. Health Informat.*, 2014, to be published.
- [71] C. Brueser, S. Winter, and S. Leonhardt, "Robust inter-beat interval estimation in cardiac vibration signals," *Phys. Meas.*, vol. 34, pp. 123–138, 2013.
- [72] J. H. Shin, S. H. Hwang, M. H. Chang, *et al.*, "Heart rate variability analysis using a ballistocardiogram during Valsalva manoeuvre and post exercise," *Phys. Meas.*, vol. 32, pp. 1239–1264, 2011.
- [73] X. Zhu, W. Chen, K. Kitamura *et al.*, "Comparison of pulse rate variability indices estimated from pressure signal and photoplethysmogram," in *Proc. IEEE Int. Conf. Biomed. Health Informat.*, 2012, pp. 867–870.
- [74] C. Brueser, S. Winter, and S. Leonhardt, "Unsupervised heart rate variability estimation from ballistocardiograms," presented at the *7th Int. Workshop Biosignal Interpretation*, Como, Italy, 2012.
- [75] O. T. Inan and G. T. A. Kovacs, "A low noise ac-bridge amplifier for ballistocardiogram measurement on an electronic weighing scale," *Phys. Meas.*, vol. 31, pp. N51–N59, 2010.
- [76] R. Wiard, O. Inan, B. Argyres *et al.*, "Automatic detection of motion artifacts in the ballistocardiogram measured on a modified bathroom scale," *Med. Biol. Eng. Comput.*, vol. 49, pp. 213–220, 2011.
- [77] K. Pandia, S. Ravindran, R. Cole *et al.*, "Motion artifact cancellation to obtain heart sounds from a single chest-worn accelerometer," presented at the *IEEE Int. Conf. Acoust., Speech, Signal Process.*, Dallas, TX, USA, 2010.
- [78] O. T. Inan, M. Etemadi, B. Widrow *et al.*, "Adaptive cancellation of floor vibrations in standing ballistocardiogram measurements using a seismic sensor as a noise reference," *IEEE Trans. Biomed. Eng.*, vol. 57, no. 3, pp. 722–727, Mar. 2010.
- [79] I. Starr and S. Ogawa, "On the aging of the heart; why is it so much more conspicuous in the ballistocardiogram than in the pulse?" *Amer. J. Med. Sci.*, vol. 242, pp. 399–410, 1961.
- [80] O. T. Inan, G. T. A. Kovacs, and L. Giovangrandi, "Evaluating the lower-body electromyogram signal acquired from the feet as a noise reference for standing ballistocardiogram measurements," *IEEE Trans. Inf. Technol. Biomed.*, vol. 14, no. 5, pp. 1188–1196, Sep. 2010.
- [81] R. M. Wiard, O. T. Inan, L. Giovangrandi *et al.*, "Preliminary results from standing ballistocardiography measurements in microgravity," in *Proc. IEEE 35th Annu. Int. Conf. Eng. Med. Biol. Soc.*, 2013, pp. 7290–7293.
- [82] I. Starr and A. Noordergraaf, *Ballistocardiography in Cardiovascular Research: Physical Aspects of the Circulation in Health and Disease*. Philadelphia, PA, USA: Lippincott, 1967.
- [83] V. Gurev, K. Tavakolian, J. Constantino *et al.*, "Mechanisms underlying isovolumic contraction and ejection peaks in seismocardiogram morphology," *J. Med. Biol. Eng.*, vol. 32, pp. 103–110, 2012.
- [84] Y. Henderson, "The mass movements of the circulation as shown by a recoil curve," *Amer. J. Phys.*, vol. 14, pp. 287–298, 1905.
- [85] W. R. Scarborough, S. A. Talbot, J. R. Braunstein *et al.*, "Proposals for ballistocardiographic nomenclature and conventions: revised and extended: Report of committee on ballistocardiographic terminology," *Circulation*, vol. 14, pp. 435–450, 1956.
- [86] N. Westerhof, F. Bosman, C. J. De Vries *et al.*, "Analog studies of the human systemic arterial tree," *J. Biomech.*, vol. 2, pp. 121–134, 1969.
- [87] J. Palladino, J. P. Mulier, F. Wu, *et al.*, "Assessing in the state of the circulatory system via parameters versus variables," *Cardiovasc. Diagn. Proc.*, vol. 13, pp. 131–139, 1996.
- [88] O. T. Inan, M. Etemadi, A. Paloma *et al.*, "Non-invasive cardiac output trending during exercise recovery on a bathroom-scale-based ballistocardiogram," *Physiol. Meas.*, vol. 30, pp. 261–274, 2009.
- [89] M. Etemadi, O. T. Inan, L. Giovangrandi *et al.*, "Rapid assessment of cardiac contractility on a home bathroom scale," *IEEE Trans. Inf. Technol. Biomed.*, vol. 15, no. 6, pp. 864–869, Nov. 2011.
- [90] E. Pinheiro, O. Postolache, and P. Girao, "Pulse arrival time and ballistocardiogram application to blood pressure variability estimation," in *Proc. IEEE Int. Workshop Med. Meas. Appl.*, 2009, pp. 132–136.
- [91] R. Casanella, J. Gomez-Clapers, and R. Pallas-Areny, "On time interval measurements using BCG," in *Proc. IEEE Annu. Int. Conf. Eng. Med. Biol. Soc.*, 2012, pp. 5034–5037.
- [92] K. Tavakolian, G. Houlton, G. A. Durmont *et al.*, "Precordial vibrations provide noninvasive detection of early-stage hemorrhage," *J. Shock*, vol. 41, pp. 91–96, 2014.
- [93] M. Di Rienzo, E. Vaini, P. Castiglioni *et al.*, "Beat-to-beat estimation of LVET and QS2 indices of cardiac mechanics from wearable seismocardiography in ambulant subjects," in *Proc. IEEE 35th Annu. Int. Conf. Eng. Med. Biol. Soc.*, 2013, pp. 7017–7020.
- [94] S. M. Munir, R. C. Boganev, E. Sobash *et al.*, "Devices in heart failure: Potential methods for device-based monitoring of congestive heart failure," *Texas Heart Inst. J.*, vol. 35, pp. 166–173, 2008.
- [95] *ClinicalTrials.gov*. [Online]. Available: <http://clinicaltrials.gov/show/NCT01121107>
- [96] J. Zanetti and D. Salerno, "Seismocardiography: A new technique for recording cardiac vibrations. concept, method, and initial observations," *J. Cardiovasc. Technol.*, vol. 9, pp. 111–120, 1990.
- [97] A. M. Weissler, W. S. Harris, and C. D. Schoenfeld, "Systolic time intervals in heart failure in man," *Circulation*, vol. 37, pp. 149–159, 1968.
- [98] C. L. Garrard, A. M. Weissler, and H. T. Dodge, "The relationship of alterations in systolic time intervals to ejection fraction in patients with cardiac disease," *Circulation*, vol. 42, pp. 455–462, 1970.
- [99] D. M. Salerno, J. M. Zanetti, L. A. Green *et al.*, "Seismocardiographic changes associated with obstruction of coronary blood flow during balloon angioplasty," *Amer. J. Cardiol.*, vol. 68, pp. 201–207, 1991.
- [100] D. Salerno, J. M. Zanetti, L. Poliac *et al.*, "Exercise seismocardiography for detection of coronary artery disease," *Amer. J. Noninvasive Cardiol.*, vol. 6, pp. 321–330, 1992.
- [101] M. Jerosch-Herold, J. Zanetti, H. Merkle *et al.*, "The seismocardiogram as magnetic-field-compatible alternative to the electrocardiogram for cardiac stress monitoring," *Int. J. Cardiac Imag.*, vol. 15, pp. 523–531, 1999.
- [102] F. I. Marcus, V. Sorrell, J. Zanetti *et al.*, "Accelerometer-derived time intervals during various pacing nodes in patients with biventricular pacemakers: Comparison with normals," *Pacing Clin. Electrophysiol.*, vol. 30, pp. 1476–1481, 2007.
- [103] B. Silke, J. Spiers, N. Herity *et al.*, "Seismocardiography during pharmacodynamic intervention in man," *Automedica*, vol. 16, pp. 35–44, 1994.
- [104] J. R. Libonati, J. Ciccolo, and J. Glassberg, "The tei index and exercise capacity," *J. Sports Med.*, vol. 41, pp. 108–113, 2001.
- [105] J. M. Zanetti and K. Tavakolian, "Seismocardiography: Past, present, and future," presented at the *IEEE Eng. Med. Biol. Soc. Conf.*, Osaka, Japan, 2013.
- [106] E. Pinheiro, O. Postolache, and P. Girao, "Theory and developments in an unobtrusive cardiovascular system representation: Ballistocardiography," *Open Biomed. Eng. J.*, vol. 4, pp. 201–216, 2010.
- [107] O. Postolache, P. S. Girao, J. Mendes *et al.*, "Unobtrusive heart rate and respiratory rate monitor embedded on a wheelchair," in *Proc. IEEE Int. Workshop Med. Meas. Appl.*, 2009, pp. 83–88.
- [108] A. Akhbardeh, K. Tavakolian, V. Gurev *et al.*, "Comparative analysis of three different modalities for characterization of the seismocardiogram," in *Proc. IEEE Annu. Int. Conf. Eng. Med. Biol. Soc.*, 2009, pp. 2899–2903.

- 1301 [109] C. Bruser, J. Diesel, M. D. H. Zink *et al.*, "Automatic detection of
1302 atrial fibrillation in cardiac vibration signals," *IEEE J. Biomed. Health*
1303 *Informat.*, vol. 17, pp. 162–171, 2013.
- 1304 [110] L. Giovangrandi, O. T. Inan, D. Banerjee *et al.*, "Preliminary results from
1305 BCG and ECG measurements in the heart failure clinic," in *Proc. IEEE*
1306 *Eng. Med. Biol. Soc. Annu. Int. Conf.*, 2012, pp. 3780–3783.
- 1307 [111] A. I. Hernandez, F. Ziglio, A. Amblard *et al.*, "Analysis of endocardial
1308 acceleration during intraoperative optimization of cardiac resynchroniza-
1309 tion therapy," in *Proc. IEEE 35th Annu. Int. Conf. Eng. Med. Biol. Soc.*,
1310 2013, pp. 7000–7003.
- 1311 [112] A. Scano and M. Strollo, "Ballistocardiographic research in weightless-
1312 ness," *Earth-Orient Appl. Space Technol.*, vol. 15, pp. 101–104, 1985.
- 1313
- [113] G. K. Prisk and P. F. Migeotte, "Physiological insights from gravity-free
ballistocardiography," in *Proc. IEEE 35th Annu. Int. Conf. Eng. Med.*
Biol. Soc., 2013, pp. 7282–7285.
- [114] R. M. Baevsky, I. I. Funtova, E. S. Luchitskaya *et al.*, "Microgravity: An
ideal environment for cardiac force measurements," *Cardiometry Open*
Access e-J., vol. 3, pp. 100–117, 2013.
- Authors' photographs and biographies not available at the time of publication.

IEEE
PROOF

QUERIES

1322

- Q1. Author the abbreviation “EMFi” has been used for two terms, i.e., electromagnetic film and electromechanical film in the text. Please check. 1323
1324
- Q2. Author: Please provide names of all authors in place of et al. in Refs. [1], [7], [8], [11]–[15], [17]–[19], [21], [22], [24]–[29], [32], [35]–[37], [42]–[45], [49], [51]–[53], [55], [57]–[59], [61]–[63], [65], [66], [68], [69], [72], [73], [76]–[78], [81], [83], [85]–[89], [92]–[94], [99]–[103], [107]–[111], and [114]. 1325
1326
1327
- Q3. Author: Please provide the technical report number in Ref. [9]. 1328
- Q4. Author: Please provide the page range in Ref. [23]. 1329
- Q5. Author: Please update Refs. [69] and [70], if possible. 1330
- Q6. Author: Please provide the year in Ref. [95]. 1331

IEEE
Proof